

IMPERIAL COLLEGE OF SCIENCE AND TECHNOLOGY

Department of Aeronautics,

Prince Consort Road, London, SW7 2BY

I.C Aero TN 87-102

June 1987 ✓

Vortex/Boundary-Layer Interactions: Data Report.

Final Report on NASA grant NAGw-581

A.D. Cutler and P. Bradshaw

Vol 1 of 2 (text)

SUMMARY

This report summarizes the work done under NASA grant NAGw-581 "Vortex/Boundary-Layer Interactions" at the time of departure of the research assistant, Dr Cutler. The experimental methods are discussed in detail and the results are presented as a large number of figures, but are not interpreted in detail. This report should be useful to anyone who wishes to make further use of the data (which are available on floppy disc or magnetic tape) for the development of turbulence models or the validation of predictive methods. Journal papers are in course of preparation.

C O N T E N T S

	Page
1. Introduction and Objectives	2
2. Experimental Facility and Methods	4
3. Results	8
4. Conclusions	11
5. Acknowledgements	11
References	12
Appendices:	
A	15
B	34
C	37
D	44
E	48
F	50
G	52
H	57
I	60
J	64
K	70
L	78

1. INTRODUCTION AND OBJECTIVES

This is an interim report written with the objective of documenting in detail the work done under NASA grant NAGw-281 "Vortex/Boundary-layer Interactions" at the time of departure of Dr A. Cutler, the research assistant employed on the contract. Other work still in progress on this contract includes the writing and submission of a number of articles on this work to journals for publication.

The objectives of the project are described in detail in the original proposal, and have been followed closely; see also the paper by Cutler and Bradshaw (1986). In brief, the objective is to study the interaction of a strong vortex, that is one with a large value of the circulation parameter

$$\frac{(\text{vortex circulation})}{(\text{stream speed}) \times (\text{boundary layer thickness})}$$

with the boundary layer developing on a flat plate. Detailed studies in the past, for example those of Shabaka, Mehta and Bradshaw (1985), Mehta, Shabaka, Shibl and Bradshaw (1983), Westphal, Eaton and Pauley (1985), Eibeck and Eaton (1987), and Pauley and Eaton (1987), have dealt with "weak" vortices, for which this parameter is in the range 0.05 to 0.5. In the present experiment the parameter is in the range 5 to 50, which is more characteristic of many of the vortex/wing or vortex/body interactions occurring on high-speed, swept-wing aircraft flying at high angles of attack.

This report discusses in detail the test configuration, the experimental methods employed, and the data available. There is little detailed interpretation of the results - which will be found in the journal papers - but the report includes a complete set of data plots and should be useful to someone who wishes to use the data (which is available on floppy disc or magnetic tape) for the development of turbulence models or the validation of predictive methods.

Two cases have been studied in detail. Both are interactions of the trailing vortex pair produced by a delta wing, mounted at an angle of attack in the working section of a wind tunnel, with the boundary layer developing on a flat plate downstream. In both cases the nominal pressure gradient on the plate (in the absence of the vortices) is zero. In the first, "delta-wing low", case the delta wing is mounted ahead of the leading edge of the plate at a height such that the wake of the trailing edge of the wing (which connects the vortex pair) passes under the plate, while the vortices pass over the plate. In this case the the boundary layer is severely distorted by the vortices, with crossflow angles exceeding 30 degrees, and significant amounts of centre-plane boundary-layer fluid are entrained into the vortex. In the second, "delta-wing high", case the delta wing is mounted much higher in relation to the test plate, and the trailing vortices produce no more than about 15 degrees of crossflow in the boundary layer: they do not entrain significant amounts of fluid out of the boundary layer, at least in the range of streamwise positions investigated here.

2. EXPERIMENTAL FACILITY AND METHODS

The 30" x 30" open circuit wind tunnel in room E455 of the Department of Aeronautics, Imperial College was used in this study. A few months after Dr Cutler commenced work on this project, this wind tunnel was purchased from the Atmospheric Physics group, and the tunnel was substantially upgraded prior to acquisition of the data set described herein. The wind tunnel, the modifications made, and the flow quality are described in the report by Cutler and Bradshaw (1987).

The configuration of the test plate and the delta-wing vortex generator for the two flow cases (the "delta-wing low" case and the "delta-wing high" case) are shown in Figures 1(a) and 1(b). In both cases the delta wing is constructed of flat, 3 mm thick aluminium plate, 533 mm in length with a span (s) of 267 mm, and chamfered leading and trailing edges. Both wings are mounted on their supports at an angle of attack of 18 ± 0.5 degrees. The support is beneath the wing in the "delta-wing low" case, so that the wake of the support passes beneath the test plate, and above in the "delta-wing high" case, so that in either case the wake of the support does not interfere with the development of the boundary layer on the test plate. In both cases the flow over the wing is slightly modified by the presence of the support, so it is possible that the circulation contained by the vortices downstream may be a little different in the two cases. However, our flow visualization and detailed hot-wire measurements indicate that the structure of the vortices upstream of the interaction region is very similar in the two cases.

Several different experimental techniques were applied in the investigation. Simple flow-visualization techniques were used in the early stages, to learn more about the general phenomena involved and to aid in the choice of two final flow configurations. Following this, the flows were mapped out in detail, using hot-wire anemometry and pressure- and temperature-measurement techniques.

A kerosene smoke generator, which provides a stream of white kerosene vapour from a tube, and smoke-wires were used for flow visualisation. The smoke-wire technique is very simple, and consists of applying kerosene to a 0.125 mm diameter stainless steel wire and vaporizing the kerosene by passing a current (very roughly 0.5 Amps) through the wire. The kerosene oil tends to form uniformly-spaced droplets on the wire which, when heated, form regular streaks of smoke - a useful feature, permitting streamlines to be visualized - which last from 1 to 3 seconds. The smoke is usually illuminated by a spotlight or, more usefully, a plane section of the flow is illuminated by a "light box" containing a cylindrical lens which produces a thin sheet (5 to 10 mm) of white light.

Surface oil-flow visualisation was used to obtain a picture of the limiting streamlines at the test plate surface. A suspension of red chalk powder in a mixture of paraffin and a light lubricating oil is painted liberally onto the white test plate surface. When the wind tunnel is switched on, the mixture flows to form streaks on the surface which remain fixed once the paraffin has evaporated away. These streaks are then photographed through a green filter (to improve contrast).

In an experiment somewhat similar to the smoke flow visualization, heat is used to mark fluid instead of smoke by passing current (roughly 5 Amps) through one or more 0.56 mm diameter nichrome resistance wires located in the flow. The distribution of temperature, and of temperature intermittency (the fraction of the time the fluid temperature is above a threshold), is then mapped by using a fine wire, operated as a resistance thermometer. The technique is described in detail in Appendix C, and the probe is described in Appendix E.

The fluid was heated in a number of different ways to mark different parts of the flow. In one experiment, a pair of resistance wires is located 1.6 mm above the surface at the leading edge of the flat plate, so that one end of each wire is held fixed and the other end passes through a guide and over a pulley, and connects to a weight which tensions the wire. In this experiment, and a similar one with a smoke wire, the heat (or smoke) diffuses rapidly within the turbulent region of the flow and diffuses negligibly beyond the turbulent/inviscid interface, so that the turbulent boundary layer region becomes rapidly filled with heat (or smoke). In a second experiment, the delta wing is heated by resistance wires, which pass through ceramic tubes of roughly 2.5 mm diameter embedded below the surface of the delta wing near the leading and trailing edges. In a third experiment, the fluid which has just left the trailing edge of the delta wing on one side of the wing centre-line is heated by a resistance wire wound in a 2.5 mm diameter spiral. This wire is connected at one end to the tip of the delta-wing and at the other end to a stiff copper tube located on the centre-line a small distance downstream of the trailing edge. In a fourth experiment, the fluid in

the core of one vortex of the pair is heated by a 2.5 mm diameter spiral resistance wire element roughly 30 mm long, connected to small electric power sockets embedded in the delta wing 35 mm and 60 mm downstream of the leading tip. The spiral wire is carefully positioned just above the surface of the delta wing so that its axis lies along the centre of one of the vortices.

Extensive measurements with a crossed hot-wire anemometer have been made. The technique involves locally aligning the probe with the flow, and measuring two mean velocity components, three Reynolds stresses and four triple products in each of four positions 45 degrees apart in roll. These results are combined to obtain all three mean velocity components, six Reynolds stresses and ten triple products in a coordinate system aligned with the wind tunnel working section axis. A traverse mechanism similar to that described by Shayesteh and Bradshaw (1987) was used to move the probe in y, yaw, pitch and roll under automatic control of a micro-computer. A second traverse mechanism, which is described in Appendix E, was used in the boundary layer region for the "delta-wing high" case. This cannot pitch the probe, but is less intrusive and permits the probe to get a little closer to the wall. The data-acquisition technique is described in Appendix A, the probe is described in Appendix F, and a small correction for the effects of gradients in the y direction on W and uw is described in Appendix G.

Measurements of total pressure have been made by traversing a pitot probe, aligned with the mean flow direction at each point in the traverse. (Flow direction information obtained from previous hot wire traverses is used to align the probe.) Full results have only been

obtained for the "delta-wing low" case where a traverse mechanism similar to that described by Shayesteh and Bradshaw (1987) was used. The technique is described in Appendix B and the probe in Appendix F. In the "delta-wing high" case, static pressure variations outside the vortex cores are small, and total-pressure measurements would have added little to hot-wire measurements of velocity components.

Profiles of total pressure have also been obtained in the boundary layer region for both cases, using a three-tube pitot probe (yaw probe) locally aligned in yaw. Particular care was taken to determine the distance of the probe from the wall accurately, and data points are closely spaced to permit boundary-layer analysis of the flow. The traverse gear described in Appendix E was used for these measurements and the technique is described in Appendix C.

3. RESULTS

The results of the smoke-flow visualization are shown in Figures 2 to 5. In Figures 2 and 4 ("delta-wing low" and "delta-wing high" cases) smoke is introduced by four smoke wires stretched across the tunnel, which pass close to, and run parallel to, the trailing edge of the delta-wing. Kerosene oil is applied only to that part of the wires which is next to the trailing edge so that only fluid which leaves the trailing edge of the wing is marked. In Figures 3 and 5 ("delta-wing low" and "delta-wing high" cases) a pair of smoke wires is used to introduce smoke into the boundary layer. In Figures 3(a) and 5(a)-(c) the smoke is introduced just downstream of the leading edge of the flat plate by a pair of smoke wires about 1.6 mm above the surface; in Figures 3(b),(c) the smoke wires are located at $x/s=1.88$, 3.2 mm above

the surface, and in Figure 3(d) the smoke wires are located at $x/s=3.75$, again 3.2 mm above the surface: recall that the delta-wing span, s , is 267 mm.

For the smoke-flow visualisation in the "delta-wing low" case, the nominal working-section velocity is only 7 m/s, so that the boundary layer between the vortices, which remains thin as a consequence of the strong divergence in this region, is laminar or transitional at least as far as $x/s=5$. The boundary layer on either side of the vortices is fully turbulent in both the "delta-wing low" and the "delta-wing high" cases, and the centre boundary layer is turbulent in the "delta-wing high" case, where the nominal velocity is a little higher (8-10 m/s) and the boundary layer a little thicker.

The results of the surface oil-flow visualization are shown in Figure 6.

The detailed flow measurements, described below, were all made at a nominal reference speed of 16 m/s. Figures 7 to 17 show the mean flow and various statistics of the turbulence measured with a hot-wire anemometer. Figure 18 shows the total pressure measurements for the "delta-wing low" case and Figures 19 to 21 show the temperature intermittency and turbulence measurements when different parts of the upstream flow were heated. The reference temperature difference (T_{ref}) for the experiment in which the boundary layer was heated at the leading edge of the flat plate (Figure 19) was about 1.8 deg C; for

that in which the delta-wing was heated the reference temperature difference was 0.7 degrees C, and where the trailing edge was heated the reference temperature difference was 1 deg C. When the vortex core was heated (as shown in Figure 38) the reference temperature difference was about 10 deg C. Figures 22 to 31 show data obtained with the three-tube pitot, and quantities derived from these data using the boundary layer analysis program described in Appendix I. Figure 32 shows wall static-pressure measurements for both flow cases, made using surface taps (see Cutler and Bradshaw, 1987). Figures 33 to 38 show a number of comparisons between profiles of data through the centre of the vortex in the "delta-wing low" case and in the "delta-wing high" case. Finally, Figures 39 to 44 show plots of quantities derived from the hot-wire data using the programs described in Appendix J.

Most of the data are presented as contour or vector plots in the y, z plane, all made using the program CONTPLOT.FOR, described by Cutler and Giampaoli (1987). The contour plots generally have repeating patterns of lines (cycles), which allow fewer lines to be labeled since the value of a contour relative to the first line of the cycle can be easily determined by line type. In cases where the contours are too close together (near the vortex core for example) only the first line in a given cycle, which is always a continuous solid line, is plotted. Vectors are also plotted: these have the tail at the y, z position where the data were obtained, and the head at $y+SV, z+SW$, where S is a scale factor and V, W are the y, z components of the vector quantity being plotted. In addition to the contour plots

shown in this report, a large number of colour photographs have been obtained, from contour plots made on a colour terminal using a program which links with a proprietary package called DISSPLA, run on a VAX. The plots are not shown here, but the method used and the quantities plotted are described in Appendix J. Finally, all the data plotted here, or referred to in the text, are available from the authors on magnetic tape written by a VAX or 5.25" IBM PC compatible floppy discs. The data library, and the various formats in which the data is written, are described in Appendix K.

4. CONCLUSIONS

This report describes the work done on NASA contract NAGw-581 at the time of departure of the research assistant, Dr A. Cutler. The experimental methods are described in detail and the results are plotted in a comprehensive set of figures. Detailed interpretation of the data is still in progress.

5. ACKNOWLEDGEMENTS

The authors are grateful for the support provided by NASA-Ames contract NAGw-581. We would like to acknowledge the invaluable contributions of Dr. D.G. Peake, the project monitor, Messrs. D. Clark and D. Dyer, technicians, and the secretarial assistance provided by Mrs R. Fairhurst. We are particularly grateful to Dr. J.K. Eaton for his development of the colour graphics routines and for much helpful advice: his sabbatical leave from Stanford University was partly supported by a British SERC Fellowship.

REFERENCES

- BASKARAN, V. and BRADSHAW, P. (1987) Experimental investigation of a three-dimensional boundary layer on an "infinite" swept concave wing. Final Report on MoD(PE) Agreement AT/2037/0243, "Research on three-dimensional shear layers".
- BRADSHAW, P. (1971) An Introduction to Turbulence and Its Measurement. Pergamon Press.
- BRADSHAW, P. (1973) Aerodynamics equipment instruction manual. I.C. Aero TN 73-105; updated Sept. 1985.
- BRADSHAW, P. (1976) Aerodynamics equipment instruction manual - part II. I.C. Aero TN 76-101; updated Sept. 1985.
- BREDERODE, V. de and BRADSHAW, P. (1974) A note on the empirical constants appearing the logarithmic law for turbulent wall flows. I.C. Aero Report 74-03.
- BRYER, D.W., and PANKHURST, R.C. (1971) Pressure-probe methods for determining wind speed and flow direction. Her Majesty's Stationery Office.
- COLES, D.E. (1962) The turbulent boundary-layer in a compressible fluid. Rand Corp. Rep. R-403-PR.
- COUSTEIX, J. (1982) Integral methods and turbulence models applied to three-dimensional boundary layers. ONERA TP 1982-13 (also presented at the IUTAM Symposium on "Three-dimensional turbulent boundary layers", 1982)
- CUTLER, A.D., and BRADSHAW, P. (1986) The interaction between a strong longitudinal vortex and a turbulent boundary layer. AIAA-86-1071.

- CUTLER, A.D., and BRADSHAW, P. (1987) The 30" x 30" wind tunnel.
I.C. Aero Report 87-01.
- CUTLER, A.D., and GIAMPAOLI, R. (1987) GENPLOT and CONTPLOT plotting
programs for Hewlett-Packard and compatible plotters.
I.C. Aero TN 87-101.
- EIBECK, P.A. and EATON, J.K. (1987) Heat transfer effects of a
longitudinal vortex imbedded in a turbulent boundary layer.
J. Heat Transfer 109, 16-24.
- GILLIS, J.C., JOHNSTON, J.P., KAYS, W.M., and MOFFAT, R.J. (1983)
Turbulent boundary layer on a convex, curved surface. Report
HMT-31, Thermosciences Div., Dept. of Mech. Engrg.,
Stanford Univ. (also NASA CR-3391).
- HOFFMANN, P.H. (1981), The "WOMBAT" constant-temperature hot wire
anemometer. I.C. Aero TN 81-102.
- KLINE, S.J., CANTWELL, B.J. and LILLEY, G.M. eds.(1981) Proceedings
of the 1980-81 AFOSR-HTTM-Stanford Conference on Complex
Turbulent Flows, Vol. I, Thermosciences Div., Dept. of Mech.
Engrg., Stanford Univ.
- LEIBOVICH, S. (1978) The structure of vortex breakdown. Ann.
Rev. of Fluid Mech. 10, pp. 221-246.
- MEHTA, R.D., SHABAKA, I.M.M.A., SHIBL, A., and BRADSHAW, P. (1983)
Longitudinal vortices imbedded in turbulent boundary layers.
AIAA-83-0378.
- MURLIS, J., TSAI, H.M. and BRADSHAW, P. (1982) The structure of
turbulent boundary layers at low Reynolds numbers.
J. Fluid Mech. 122, 13-56.

- PAULEY, W.R. and EATON, J.K. (1987) An experimental study of the development of longitudinal vortex pairs embedded in a turbulent boundary layer. AIAA paper no. 87-1309.
- PIERCE, F.J., McALISTER, J.E. and TENNANT, M.H. (1983) Near-wall similarity in a pressure-driven three-dimensional turbulent boundary layer. J. Fluids Eng. 105, pp. 257-262.
- SHABAKA, I.M.M.A., MEHTA, R.D. and BRADSHAW, P. (1985) Longitudinal vortices imbedded in turbulent boundary-layers. Part 1. Single vortex. J. Fluid Mech. 155, pp. 37-57.
- SHAYESTEH, M.V., and BRADSHAW, P. (1987) Microcomputer-controlled traverse gear for three-dimensional flow explorations. J. Phys. E: Sci. Instrum. 20, pp. 320-322.
- SPALDING, D.B. (1961) A single formula for the "law of the wall". J. Appl. Mech. 28, pp. 455-457.
- SUBRAMANIAN, C. S., and BRADSHAW, P. (1985) On-line processing of turbulent signals using the Advance 86 (IBM PC compatible) computer. I.C. Aero TN 85-101.
- WESTPHAL, R.V., EATON, J.K. and PAULEY, W.R. (1985) Interaction between a vortex and a turbulent boundary-layer in a streamwise pressure gradient. Proc. 5th Sympo. Turbulent Shear Flows, Cornell Univ., pp. 1-8.

Appendix A

Crossed Hot-Wire Calibration and Data Acquisition.

A.1 Introduction

The method of calibration of a crossed hot-wire (x-wire) and acquisition of profiles of data using the program HWTRAV.FOR or HWTRV1.FOR is described. We also discuss the manner in which the data are converted from a coordinate system orthogonal to the probe axis to a coordinate system orthogonal to the wind tunnel axis using the program PROCESS.FOR.

The program HWTRAV.FOR was written to obtain data using the mechanism described by Shayesteh and Bradshaw (1987) which has four motorized and computer controllable movements - y, yaw, pitch and roll. The program traverses the x-wire through a sequence of y positions and at each position the probe axis is approximately aligned with the local mean flow. The probe is assumed to be mounted in the traverse mechanism in such a way that, when the probe is pitched or yawed, the centre of the probe measuring volume remains fixed in space. A second version, HWTRV1.FOR, has been written to control the traverse mechanism described in Appendix D, which has motorized y and yaw movements but no pitching movement, and is for use in flows whose pitch angle is small (< 5 degrees).

A.2 Instrumentation Requirements

A microcomputer manufactured by Seattle Computer Products and based on the S-100 bus is used for the acquisition of the data and control of the traversing mechanism. The computer is equipped with the SCP200B processor board which is based on the Intel 8086 CPU chip with an 8087 coprocessor and 8MHz clock, an SCP300F CPU Support Board which includes eight-bit parallel input and output ports, the SCP400 Multi-port Serial Card, and 448 kB of static RAM. Data storage is provided by a pair of 8" dual-sided double-density floppy disk drives and a Tarbell Double Density Floppy Disk Interface giving 1.2 MB storage per disk. Data acquisition is with a Dual Systems AIM-12 12-bit A/D converter board operated in differential mode, giving 16 analog channels. The microcomputer runs a simple version of the Microsoft Disc Operating System (MS-DOS version), and we use the Microsoft FORTRAN compiler and linker.

Figure A.1 is a block diagram showing the instrumentation. The I.C Aeronautics Department PHI system is used (see Bradshaw, 1973 and 1976) where specialized modules manufactured in-house plug into a power supply rack.

The hot-wire probe is connected by a pair of 5 metre coaxial cables to two Wombat hot-wire bridges (Hoffmann, 1981). The output from these goes to a locally-made "Mottbox" amplifier and filter which subtracts about 2 volts from the signal, amplifies it (usually by a factor of 5) and then low-pass filters it at a 20kHz cutoff. This is

so that the fluctuating signal from each hot-wire covers as much as possible of the -10V to +10V range of the A/D converter, without exceeding it. The A/D converter resolution (the voltage step to change the A/D output by one least significant bit) is 4.9 mV so that, given a typical calibration, the velocity resolution at 16 m/s flow speed is about 0.04 m/s or 0.25 percent. The output then goes to a sample and hold PHI module (with one sample-and-hold amplifier per channel) and from there, to the A/D converter.

The computer's parallel port is used to control the traverse mechanism movements and to provide the "hold" signal to the sample and hold modules. A PHI module is used to power each of the four traverse movements. For each module two TTL signals are required, one to activate positive movement and the second to activate negative movement. Seven of the eight lines from the parallel port are connected to these modules, permitting positive and negative movement in pitch, roll and yaw, and positive movement only in the y direction (switch PHI module to manual to rewind). The eighth line provides the hold signal. Each module receives the voltage from the position potentiometer on the section of the traverse mechanism which it controls, and these voltages are fed to the A/D converter.

Finally, a Furness Controls MDC FC001 micromanometer is used to measure the flow dynamic pressure for probe calibration or to obtain a reference velocity. Its output is amplified by a factor of ten with a PHI module and then connected to the A/D converter.

A.3 Program Layout

The program HWTRAV.FOR is written to provide maximum flexibility of operation by providing tables of options at two separate levels. Upon starting the program the following Options are offered:

- 1 - Initialize traverse gear;
- 2 - obtain hot-wire channels offset/gain;
- 3 - calibrate wires;
- 4 - initialize lookup array;
- 5 - do a traverse in the y-direction;
- 6 - output the data to a file;
- 7 - new run;
- 8 - stop.

If Option 1 is chosen, the traversing mechanism current position and calibration coefficients are input. The program requires that the user input the current location of channels 1 to 4, 1 being y, 2 being yaw, 3 being pitch and 4 being roll. It then reads calibration coefficients from a file TRVDAT.DAT which must be resident in the default disk directory. The data which must be provided in this file and its format are indicated by comment statements within the program, and a sample is shown in Table A.1.

If Option 2 is chosen, then the offset voltage and gain factor provided by the "Mottbox" are evaluated by the program. The signal from the hot-wire bridge must be disconnected and two or more known

voltages be input to the two channels of offset and gain, the same voltage being applied to each channel. The user then types in the voltage at the computer terminal.

If Option 3 is chosen, then the x-wire probe is calibrated for velocity response and, optionally, for yaw response. The calibration gives as its outputs the coefficients for the King's law fit of bridge voltage to wire velocity and the wire angles relative to the probe axis. If the yaw calibration is not performed then wire angles from the last yaw calibration are used. The calibration procedure is described in Section A.4.

If Option 4 is chosen, then the program evaluates the terms in two lookup arrays of dimension 4096, one for each wire. The array index is the voltage measured by the A/D converter as a number of least significant bits, and the array value is the corresponding effective cooling velocity multiplied by the cosine of the wire angle (i.e. $u_{eff}\cos(\psi)$, where ψ is defined in Figure 2(d)). The array values are determined from the King's law coefficients obtained in the calibration procedure described in Section A.4 below.

If Option 5 is chosen, then a second Option list is presented which permits the various tasks related to data acquisition, described in Section A.5, to be performed.

If Option 6 is chosen, all the data obtained since the last write-to-file or the last time Option 7 was selected are written to a

data file in a format which can be read by the program PROCESS.FOR. The output data include probe y position, yaw and pitch angles, the three components of mean velocity, the six Reynolds stresses and the ten triple products, all measured in a coordinate system orthogonal to the probe axis (indicated by the subscript p in Figure A.2).

Option 7 resets the data-point count to zero.

Option 8 ends the program.

Note that Options 1, 2, 3 and 4 must be selected, in that order, before data can be obtained. Any Option may be selected subsequently, so that for example, the probe may be recalibrated without reinitializing the traverse mechanism.

A.4 Calibration

The probe is calibrated in the freestream of the working section flow. It is assumed that the yaw and pitch angle zeros are with the probe axis parallel to the wind tunnel axis and that the flow at the calibration point is also parallel to the axis. The sense of the x, y, z coordinate system, the yaw and pitch angles and the roll position is defined by Figure A.2. The wires are calibrated in roll position 2 so that the wires lie in the plane of yaw.

The program requires that the pressure transducer calibration coefficient be typed in, in units of Volts/(m/s)², and then that the

pressure transducer be connected to measure zero pressure difference to find the zero. The pressure transducer is then connected to a pitot probe located in the freestream and a static tap near the x-wire to measure the dynamic pressure at the x-wire probe. The flow speed in the tunnel is set by the operator, allowed to settle and the program measures the velocity U and hot-wire bridge voltages E for each wire. This is repeated for a total of from two to ten times and the results are least-squares fitted to the King's law function $E^2 = A + BU^n$. The user inputs the exponent n at the terminal, but has the opportunity to change it so that the fit to the data can be optimized. The fits with n in the range 0.40 to 0.45 are always very good if the probe is in good condition, with correlation coefficient of fit usually better than 0.99990.

The wire angles are obtained by yawing the probe through a sequence of angles ($\theta_y = 0, -15, -10, -5, 0, 5, 10, 15$, and 0 degrees) and fitting the response to a cosine cooling law, following Bradshaw (1971). The cosine cooling law is $U_{eff,1} = U \cos(\psi_1 + \theta_y)$ for wire 1 and $U_{eff,2} = U \cos(\psi_2 - \theta_y)$ for wire 2, where U_{eff} is an effective cooling velocity for the wire, and these expressions may be rewritten in the following manner:

$$-U_{eff,1}/U_{eff,1}(\theta_y = 0) + \cos(\theta_y) = \tan(\psi_1) \sin(\theta_y)$$

$$-U_{eff,2}/U_{eff,2}(\theta_y = 0) + \cos(\theta_y) = -\tan(\psi_2) \sin(\theta_y).$$

The calibration data $-U_{\text{eff}}/U_{\text{eff}}(\theta_y = 0) + \cos(\theta_y)$ are least squares fit to the linear function $a \sin(\theta_y) + b$ giving a which is the tangent (or minus the tangent) of the effective wire angle (b should be zero). The calibration data are found to fit this function very well if the wire is in good condition, with correlation coefficient of fit usually better than 0.99950. The geometrical angles of the wires need not be measured.

A.5 Data Acquisition

If option 5 is chosen, the operator is requested to connect the pressure transducer to the reference dynamic pressure, and is then given the following Options:

- 0 - Return the reference velocity
- 1 - return location of specified channel
- 2 - move the probe
- 3 - quick mean velocity measurement
- 4 - u and v statistics
- 5 - align the probe with the flow
- 6 - data taking sequence (4 roll angles)
- 7 - automated y-traverse with data taking
- 8 - return to primary Options

If Option 0 is chosen, the reference velocity (the velocity obtained from a pitot tube in the free stream and a reference static

tap) is measured and output to the terminal. This velocity will subsequently be used to non-dimensionalise all the data written to disc file.

If Option 1 is chosen, the location of a selected traverse mechanism degree of freedom is output to the terminal.

If Option 2 is chosen, the selected traverse mechanism degree of freedom is moved to a target value input by the user. In all traverse mechanism movements, the program ensures that the traverse mechanism always approaches its final position in the same direction (the direction of positive movement), so that there are no problems of backlash and probe positioning is accurately repeatable whatever the initial probe position.

If Option 3 is chosen, the program returns U_w and V_w , that is the mean velocity component parallel to the probe axis and the mean velocity component normal to the probe axis in the plane of the crossed wires. The program obtains 2000 voltage samples from each of the two hot-wires, which are then converted to effective wire cooling velocities using the lookup table described in Section A.3 above. The mean cooling velocities for each wire, $U_{eff,1}$ and $U_{eff,2}$ are found by summing the individual samples. The following expression is then used to convert these to U_w and V_w :

$$U_w = (U_{eff,1} \tan(\psi_2) + U_{eff,2} \tan(\psi_1)) / (\tan(\psi_1) + \tan(\psi_2))$$

$$V_w = (U_{eff,1} - U_{eff,2}) / (\tan(\psi_1) + \tan(\psi_2)).$$

If Options 4, 6 or 7 are chosen, all of which involve the evaluation of turbulence statistics, the program first requests the user to input the number of data samples per channel to be taken to form the averages (n_p). If Option 4 is chosen, the following statistics are obtained: U_w , V_w , $\overline{u^2}_w$, $(\overline{uv})_w$, $\overline{v^2}_w$, $\overline{u^3}_w$, $(\overline{u^2v})_w$, $(\overline{uv^2})_w$, $\overline{v^3}_w$, where u_w is the fluctuating component of velocity parallel to the probe axis and v_w is the fluctuating component normal to the probe axis and in the plane of the crossed wires. The method by which these statistics are obtained is described in Section A.6.

If Option 5 is chosen, the probe axis is aligned with the local mean flow direction. The velocities U_w and V_w are obtained as described in Option 3 with the wire in roll position 0, and the probe is pitched to an angle given by the following expression.

$$\theta_{z,new} = \theta_{z,old} + \tan^{-1}(V_w/U_w)$$

The probe is then rolled to position 2, U_w and V_w are again measured and the probe yawed to an angle given by the following expression.

$$\theta_{y,new} = \theta_{y,old} - \tan^{-1}(V_w/U_w)/\cos(\theta_z)$$

The probe is then rolled back to position 0 and the alignment in pitch is repeated. If the angle pitched or yawed in any of the above alignment movements exceeds 15 degrees then the whole process is repeated. It is found that this procedure aligns the probe axis with the local mean flow direction to within a degree, which is sufficient to obtain reliable turbulence statistics. A program Option allows alignment in pitch to be omitted, so that if the probe is near the wall a pitching movement which might cause the probe arm to collide

with the wall can be avoided. Pitching movement is also, of course, omitted by the program HWTRV1.FOR.

If Option 6 is chosen, the above statistics are obtained in roll positions 0, 1, 2, 3 and the reference velocity is obtained. The results are then combined in the following manner to give three mean velocities, six Reynolds stresses and ten triple products in a coordinate system aligned with the probe axis - that is, referring to Figure A.2, x_p is parallel to the probe axis, y_p is in the plane of x_y and y , and $z_p = z_y$.

$$U_p = (U_{w,0} + U_{w,1} + U_{w,2} + U_{w,3})/4$$

$$V_p = V_{w,0}$$

$$W_p = V_{w,2}$$

$$\overline{u^2}_p = (\overline{u^2}_{w,0} + \overline{u^2}_{w,1} + \overline{u^2}_{w,2} + \overline{u^2}_{w,3})/4$$

$$\overline{v^2}_p = \overline{v^2}_{w,0}$$

$$\overline{w^2}_p = \overline{v^2}_{w,2}$$

$$(\overline{uv})_p = (\overline{uv})_{w,0}$$

$$(\overline{uw})_p = (\overline{uv})_{w,2}$$

$$(\overline{vw})_p = (\overline{v^2}_{w,1} - \overline{v^2}_{w,3})/2$$

$$\overline{u^3}_p = (\overline{u^3}_{w,0} + \overline{u^3}_{w,1} + \overline{u^3}_{w,2} + \overline{u^3}_{w,3})/4$$

$$\overline{v^3}_p = \overline{v^3}_{w,0}$$

$$\overline{w^3}_p = \overline{v^3}_{w,2}$$

$$(\overline{u^2v})_p = (\overline{u^2v})_{w,0}$$

$$(\overline{u^2w})_p = (\overline{u^2v})_{w,2}$$

$$(\overline{uv^2})_p = (\overline{uv^2})_{w,0}$$

$$(\overline{uw^2})_p = (\overline{uv^2})_{w,2}$$

$$(\overline{v^2w})_p = (\sqrt{2}(\overline{v^3}_{w,1} + \overline{v^3}_{w,3}) - \overline{v^3}_{w,2})/3$$

$$(\overline{vw^2})_p = (\sqrt{2}(\overline{v^3}_{w,1} - \overline{v^3}_{w,3}) - \overline{v^3}_{w,0})/3$$

$$(\overline{uvw})_p = ((\overline{uv^2})_{w,1} - (\overline{uv^2})_{w,3})/2$$

These results plus y , θ_y , θ_z are added to the results data array and the "number of data points acquired" index is incremented.

If Option 7 is chosen, the probe is traversed in the y direction through a sequence of points; at each point the probe is aligned with the local flow direction as for Option 5 and data are taken as for Option 6. The program requires that the sequence of y values be input by the user at the terminal before the traverse commences. The operation is then fully automatic.

Finally, if Option 8 is chosen then the program returns to the primary Option list.

A.6 Calculation of Turbulence Statistics

This section describes the method of evaluation of turbulence statistics used when Options 4, 6 or 7 above are selected. In evaluating these quantities, particular attention has been paid to ensuring that the results are not affected by computer roundoff error (32-bit arithmetic).

For each voltage sample from each of the hot-wire bridges an instantaneous effective cooling velocity is obtained by reference to the lookup table (Option 4 in Section A.3). The effective cooling velocities for the two wires are converted to an instantaneous velocity with component u_w parallel to the probe axis and component v_w

normal to the axis (in the plane of the crossed wires) by using the following equations.

$$u_w = (u_{\text{eff},1} \tan(\psi_2) + u_{\text{eff},2} \tan(\psi_1)) / (\tan(\psi_1) + \tan(\psi_2))$$

$$v_w = (u_{\text{eff},1} - u_{\text{eff},2}) / (\tan(\psi_1) + \tan(\psi_2))$$

The velocities $u_{w,\text{ref}}$ and $v_{w,\text{ref}}$, where the subscript ref indicates the first sample from the sequence of u_w and v_w to be averaged, are subtracted from the first and subsequent u_w and v_w samples. This is done because, in cases where the turbulence intensity is low, the fluctuating component contribution to the sum of the second and third order products of these quantities would otherwise be small compared to the mean component contribution. In this case, any small accumulated computer roundoff error incurred in evaluating the sums might not be small compared to the fluctuating contribution, and therefore lead to a relatively large error in the statistics of the fluctuations. These velocities, their second and third order products are summed in blocks of one hundred, and these blocks are themselves summed as indicated in the equations below.

$$S_i = \sum_{j=1}^{100} u_i + \sum_{j=101}^{200} u_i + \dots + \sum_{j=1}^{n_p} u_i$$

$$S_{ij} = \sum_{j=1}^{100} u_i u_j + \sum_{j=101}^{200} u_i u_j + \dots + \sum_{j=1}^{n_p} u_i u_j$$

$$S_{ijk} = \sum_{j=1}^{100} u_i u_j u_k + \sum_{j=101}^{200} u_i u_j u_k + \dots + \sum_{j=1}^{n_p} u_i u_j u_k$$

where $i, j, k = 1$ or 2 , $u_1 = u_w - u_{w,ref}$ and $u_2 = v_w - v_{w,ref}$. The sums are formed in this manner to avoid a large accumulation of roundoff error, which will occur when a sum becomes so large that the value of the quantity being repeatedly added to the sum is of the order of the roundoff error incurred in performing the addition. Other schemes for avoiding this problem have been suggested, but this one is simple and minimizes the number of additional mathematical operations required, an important consideration since we wish to minimize program execution time.

Finally, U_w , V_w , $\overline{u^2}_w$, \overline{uv}_w , $\overline{v^2}_w$, $\overline{u^3}_w$, $(\overline{u^2v})_w$, $(\overline{uv^2})_w$ and $\overline{v^3}_w$ are determined from the above sums by using the following equations.

$$U_i = S_i/n_p + u_{i,ref}$$

$$\overline{u_i u_j} = S_{ij}/n_p - U_i U_j$$

$$\overline{u_i u_j u_k} = S_{ijk}/n_p - U_i \overline{u_j u_k} - U_j \overline{u_i u_k} - U_k \overline{u_i u_j} - U_i U_j U_k$$

It takes 10 or 15 seconds to obtain 10000 samples, and sums are formed whilst data is taken, so that there is little additional overhead incurred in forming the statistics. We recommend that from 5000 to 20000 samples per wire (n_p) be taken to obtain stationary averages - note that we used 18000 samples per wire in the hot-wire measurements described in the main body of this report.

A.7 Post-Processing Turbulence Results

The turbulence results written by the program HWTRAV.FOR to data file have been measured in a coordinate system which is locally aligned with the crossed wire probe axis, and is different for each y position in the traverse since the probe pitch and yaw angles change. The program PROCESS.FOR was written to read data from files written by HWTRAV.FOR, to convert the data to a coordinate system orthogonal to the wind tunnel axis and then output the data for a number of traverses to a data file.

The conversion from the local probe orthogonal coordinate system (x_p, y_p, z_p) to the wind tunnel orthogonal system (x, y, z) is done by evaluating the following expressions which we have written in tensor notation (ie. repeated indices are summed from 1 to 3, and $u_1 = u$, $u_2 = v$, and $u_3 = w$):

$$\begin{aligned} u_i &= a_{ij} (u_j)_p \\ \overline{u_i u_j} &= a_{ikl} (\overline{u_k u_l})_p \\ \overline{u_i u_j u_k} &= a_{il} a_{jm} a_{kn} (\overline{u_l u_m u_n})_p \end{aligned}$$

where $a_{11} = \cos(\theta_z)\cos(\theta_y)$, $a_{12} = -\sin(\theta_z)\cos(\theta_y)$, $a_{13} = \sin(\theta_y)$,

$$a_{21} = \sin(\theta_z), \quad a_{22} = \cos(\theta_z), \quad a_{23} = 0, \quad a_{31} = \cos(\theta_z)\sin(\theta_y),$$

$$a_{32} = \sin(\theta_z)\sin(\theta_y) \quad \text{and} \quad a_{33} = \cos(\theta_y).$$

Certain versions of PROCESS.FOR may also implement corrections for the effect of y gradients of mean flow and Reynolds stresses on W and uw . These corrections are described in Appendix G.

The program then outputs the results in a choice of two different formats. The first is a simple format which is suitable to be read by a plotting or a data analysis program but is not self-explanatory; the user needs to refer to PROCESS.FOR to determine how the data are written in the file. The second contains text as well as the data, and is laid out carefully so as to be suitable for inclusion in a report. The program also has the option of outputting to a file the yaw and pitch angles required at each given y location to align a probe exactly with the local mean flow direction. This information is used by the data acquisition program DLPTRV.FOR described in Appendix B.

Volt/in	Volt per second	Tolerance (volts)	Max Voltage	Min Voltage
0.504	-0.0256	0.001	6.0	1.0
0.0102	-0.0212	0.005	5.5	1.0
0.0363	0.23	0.008	5.5	1.5
0.5781	-0.548	0.050	6.0	0.

Table A.1.

Sample TRVDAT. DAT data file.

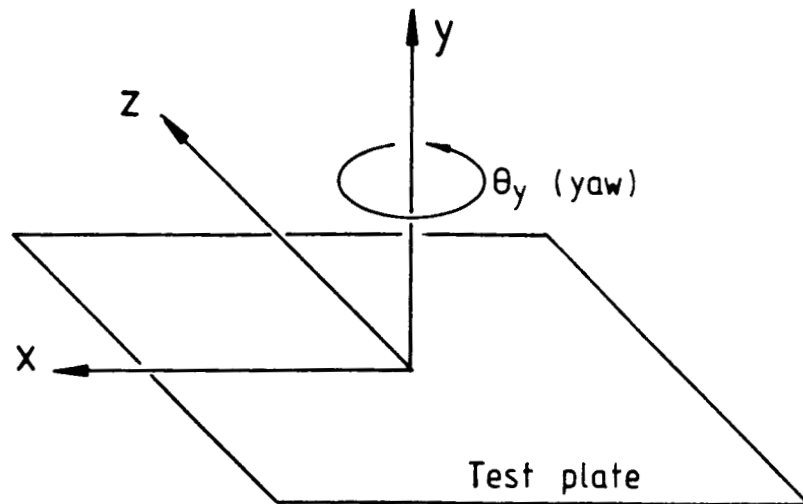
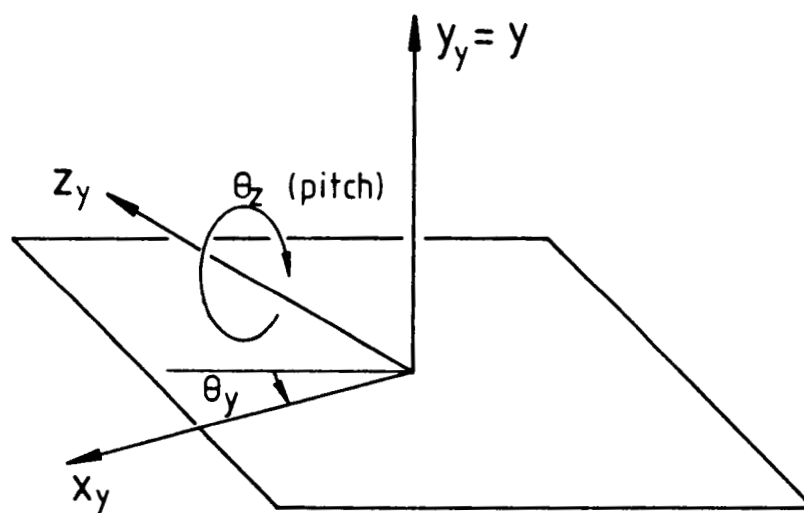


Figure A.2 Definition of axes
(a) with respect to tunnel axis



(b) with respect to hot-wire probe axis

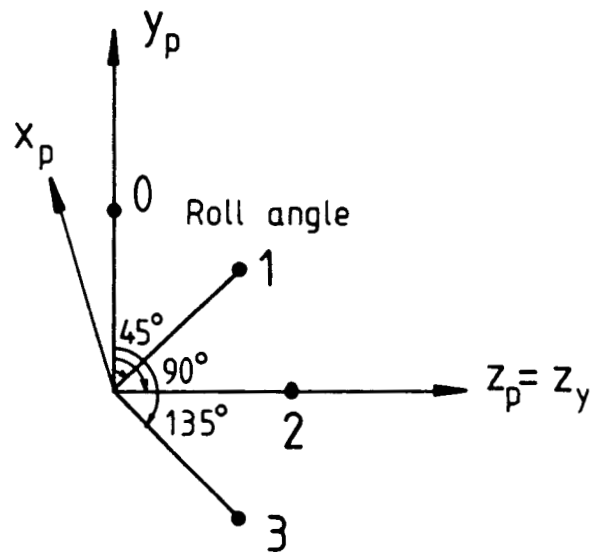


Figure A.2(c) Definition of probe roll sequence

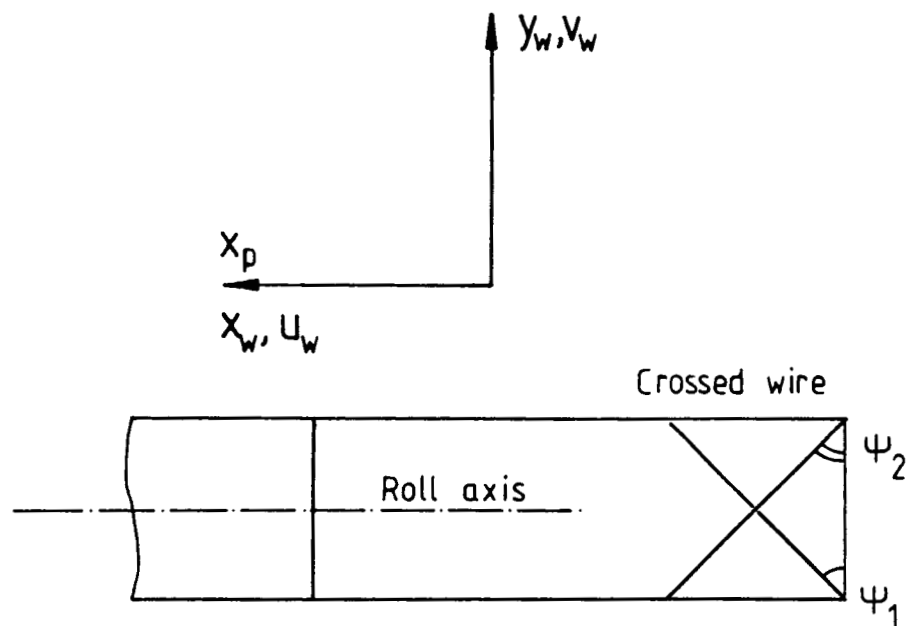


Figure A.2(d) Components in plane of crossed wires.

Appendix B

The Acquisition of Total Pressure Data.

B.1 Introduction

This Appendix describes the program DLPTRV.FOR which has been written to acquire total pressure data using the traversing mechanism described by Shayesteh and Bradshaw (1987). It is similar to the hot-wire data acquisition program described in Appendix A, and much of the programming which controls the traversing mechanism is the same, as are the instrumentation requirements. The program style, in which the user is presented with an Option list upon the completion of each program task, is also similar and so we will not describe the operation of the program in the same detail.

B.2 Instrumentation Requirements

There are no additional instrumentation requirements to those described in Section A.2 for the hot-wire data acquisition. The hot-wire bridge and sample-and-hold modules are of course redundant, but need not be removed. The hot-wire probe is replaced by a total pressure tube which is straight and carefully positioned in its holder so that movement of the traverse mechanism in yaw or pitch causes the probe to pivot in such a way that the probe tip remains fixed in space.

B.3 Program Layout

When the program is started, the user is requested to input n_p , the number of pressure data samples used to form the averages, to input the pressure transducer calibration coefficient in Volts/(m/s)², and then to connect the pressure transducer to zero pressure so that the pressure transducer zero may be measured. Following this, an Option list is presented:

- 1 - Initialise traverse gear;
- 2 - get reference dynamic pressure;
- 3 - move the probe;
- 4 - do a traverse in the y-direction;
- 5 - output the data to a file;
- 6 - new run;
- 7 - stop.

Option 1 is the same as Option 1 described in Section A.3.

If Option 2 is chosen, the pressure difference connected to the pressure transducer is returned in units of (m/s)², and subsequently used as a reference pressure for the data output to disc file.

If Option 3 is chosen, the probe is moved (in y, yaw, or pitch) to a position which the user inputs. The program takes no account of backlash in the yaw or pitch movement gears, but pitch and yaw angles will not be in error by more than about one degree as a result. The pitot probe needs to be aligned with the local mean flow to within no more than about +5 degrees to obtain accurate measurements of total pressure, so that this misalignment error is not important.

If Option 4 is chosen, the probe is traversed in the y direction, and total pressure data are obtained at a series of points under automatic control of the computer. The program requires that, for each point in the traverse, the y position and the yaw and pitch angles required to align the probe with the local mean flow position be input before the traverse commences. This information may be input at the terminal or may be read from a data file. A suitable data file is created by the program PROCESS.FOR, which calculates the required yaw and pitch angles at the previously used y positions from the data obtained in a traverse with a crossed hot-wire at the same x and z location. The user is then requested to connect the pressure transducer to the pitot probe (and an appropriate reference static pressure) and n_p pressure samples are obtained at each y. These are averaged to minimize the accumulation of computer roundoff error by using the following expression:

$$P_{ave,i+1} = P_{ave,i} + (p_{i+1} - P_{ave,i})/(i+1);$$

where $P_{ave,1} = p_1$, $i=1, \dots, n_p$ and $P_{ave,np}$ is the final average pressure. The y position and corresponding pressure for each point are then added to a results array.

If Option 5 is chosen, the program writes the contents of the results array into a data file in a simple format, with the pressures non-dimensionalised on the reference pressure obtained using Option 2.

If Option 6 is chosen, the number of points in the results array counter is set to zero, and if Option 7 is chosen the program stops.

Appendix C

The Acquisition of Boundary Layer Profiles with a Three-hole Pitot Probe.

C.1 Introduction

This Appendix describes the program 3HLTRV.FOR which was written to acquire profiles of mean total pressure and cross-flow angle in a boundary layer with a significant cross-flow but with small pitch. The traverse mechanism described in Appendix D, which has motorized y and yaw movements, and a three-tube probe of the type shown in Figure 46(d) of Bryer and Pankhurst (1971) are used.

C.2 Instrumentation Requirements

The instrumentation requirements are the same as in Section B.2, but with the addition of a second pressure transducer, the output of which is amplified and connected to the computer A/D through the distribution box. The first pressure transducer (number 1) will be connected to the central tube of the probe to measure dynamic pressure and the second (number 2) will be connected to measure the pressure difference between the side tubes. For more precise details of the connections between the computer A/D or parallel port and the pressure transducers or traverse mechanism modules, the user should refer to the program listing.

C.3 Program Layout

When the program is run, the user is asked to input the diameter of the tubes in the probe, D , and is then given the following options, where "dp" denotes a pressure difference:

- 1 - Initialize traverse gear;
- 2 - calibrate pressure transducers;
- 3 - yaw calibration;
- 4 - obtain dp reference;
- 5 - obtain dp static;
- 6 - return probe location;
- 7 - move probe;
- 8 - null alignment;
- 9 - find the wall;
- 10 - data taking traverse;
- 11 - start again;
- 12 - output data to a file;
- 99 - stop.

If Option 1 is chosen, the user is requested to input the current y position and yaw angle. Note that the yaw angle zero lies, by definition, parallel to the tunnel axis. The program then reads calibration data from a file TRVDAT1.DAT which must be resident on the default disc drive and whose contents and format are given in the program listing.

If Option 2 is chosen, the user is requested to input n_p , the number of samples used to form averages, and the calibration coefficient for pressure transducer 1 in $\text{Volts}/(\text{m/s})^2$. Both pressure transducers should be connected to zero pressure difference and the program obtains the zero reading. All pressure measurements made by the program are obtained using the same program subroutine, which forms averages using the algorithm described in Section B.3.

If Option 3 is chosen, the probe should be located in the freestream of a calibration flow (one which is parallel to the tunnel axis) and near to a static tap so that the dynamic pressure at the probe tip may be obtained. Pressure transducer 1 is then connected to the pressure difference between the centre tube of the probe and the nearby static tap ($p_1 - p$), and pressure transducer 2 is connected to the pressure difference between the side tubes of the probe ($p_3 - p_2$). The probe is then yawed through the angles $\theta_{y,c} = -20, -15, -10, -5, 0, 5, 10, 15, 20$ degrees, and at each location the outputs of pressure transducers 1 and 2 are measured. The angle $\theta_{y,c}$ and non-dimensional pressure difference $(p_3 - p_2)/(p_1 - p)$ are stored in an array for future use. Subsequent options assume the probe is located in the flow for which measurements are desired.

If Option 4 is chosen, pressure transducer 1 should be connected to the pressure difference between a reference static tap and a pitot probe located in the freestream, and the pressure difference is measured. This will subsequently be used to normalize the results when output to disc file.

If Option 5 is chosen, pressure transducer 1 should be connected to measure the pressure difference between the static tap at the same x, z as the traverse (making sure that the probe is out of the way and the static pressure is therefore not modified by the presence of the probe) and the reference static tap. This pressure difference is measured and will be needed subsequently to calculate velocities from the total pressure measured by the centre tube.

If Option 6 is chosen, the program will return the current position of the probe in y or the yaw angle.

If Option 7 is chosen, the program will move the probe in y or yaw to a position input by the user at the terminal.

If Options 8, 9 or 10 are chosen, pressure transducer 1 should be connected to the pressure difference between the centre tube and the reference static tap ($p_1 - p$) and pressure transducer 2 should be connected to the pressure difference between the two side tubes in the same manner as for Option 3 ($p_3 - p_2$).

If Option 8 is chosen, the program measures the output from pressure transducers 1 and 2 to give the ratio $(p_3 - p_2)/(p_1 - p)$. The angle through which the probe should be yawed to align with the flow is given by the following expression

$$\theta_{y,new} - \theta_{y,old} = -\theta_{y,c}((p_3 - p_2)/(p_1 - p)),$$

where the right hand side is evaluated by a piecewise linear fit to the calibration data. If this angle is less than 0.5 degrees then the probe is assumed to be adequately aligned with the flow, the cross-flow angle is then simply $\theta_{y,new}$, and the dynamic pressure $P-p_1=p_1-p$. If this angle is greater than 0.5 degrees, the probe is yawed to the angle $\theta_{y,new}$ and the procedure repeated.

If Option 9 is chosen, the user is requested to input the y step for the wall search (y_s , a small distance of the order 0.002 inches) and to locate the probe so that its tip just touches the wall. The program then instructs the traverse mechanism to move the probe out from the wall a distance y_s , aligns the probe in yaw as in Option 8 above, and asks the user if the probe tip has moved off the wall. If it has not, the procedure is repeated until the slack in the traverse gear is taken up and spring in the probe tip (which is bent a small amount by contact with the wall) is released, at which time the probe tip begins to lift off the wall. The point at which the probe lifts off the wall can easily be detected by inspection of the dynamic pressure measurements (these are output to the terminal by the program) or by inspection of the probe tip itself. Gaps less than 0.001 inch between the probe tip and the wall can be detected in this manner. When the probe tip has lifted off the wall and the user has answered the above question in the affirmative, the probe is moved out one further step y_s and the dynamic pressure and flow yaw angle are obtained once more. The y position at which the probe just touches the wall (y_w) is determined from the dynamic pressure when the probe was last touching the wall (P_a-p_{ref}) and from the y and dynamic pressure at the two

points when the probe tip is away the wall (y_b , $P_b - P_{ref}$, y_c , and $P_c - P_{ref}$) using the expression

$$y_{wall} = y_b - (y_c - y_b)(P_b - P_a)/(P_c - P_b).$$

If this expression does not give y_{wall} in the range $y_a < y_{wall} < y_b$ (which we know to be the case) then y_{wall} is set equal to y_a , or y_b , whichever is closer to the value given by the above expression. The y calibration for the traverse mechanism and the values y_a , y_b and y_c are corrected so that y becomes $y + D/2 - y_{wall}$, the distance of the center of the probe from the test surface accurate to within y_s . The measurements obtained above are the first three points in the results data array and the number of points in the data array counter (n_t) is three.

If Option 10 is chosen, the probe is traversed in the y direction, and total pressure and yaw angle data are obtained at a series of points under automatic control of the computer. The user has the option of inputting a sequence of y values for the traverse at the terminal or having the computer calculate a sequence which would be suitable for a boundary layer traverse. If the latter alternative is chosen, the user is requested to input a rough estimate of the boundary layer thickness (δ_{995}), the maximum y in the traverse (y_{max}), and the initial step (dy_1). The program then determines the present y location (y_1) and calculates a sequence of y values (y_i , $i=1, \dots$) as follows:

$$y_{i+1} = y_i + dy_i$$

provided

$$y_{i+1} < y_{\max}$$

where

$$dy_i = y_i/y_1 dy_1 \text{ or } dy_i = 0.05 \delta_{995} \text{ (whichever the less).}$$

The traverse then proceeds and the results are added to the results data array, the number of points counter (n_t) being incremented.

If Option 11 is chosen, the number of points counter (n_t) is set to zero.

If Option 12 is chosen, the reference dynamic pressure ($P_{\text{ref}} - p_{\text{ref}}$) and the static pressure ($p - p_{\text{ref}}$) measured in Options 4 and 5, followed by the sequence of y , yaw angle θ_y and total pressure coefficients $(P - p_{\text{ref}})/(P_{\text{ref}} - p_{\text{ref}})$ are output to a disc file. Before this, however 0.18D is added to y to correct for the displacement of the effective position of the probe centre as a result of mean shear (following Young and Maas, 1936).

If Option 99 is chosen, the program stops.

Note that Options 1 to 3 must be selected in that order before any data can be acquired, and Options 4 and 5 must have been selected before any attempt is made to write the results to a disc file.

Appendix D

The Acquisition of Temperature Intermittency Data

D.1 Introduction

This Appendix describes the program INTTRV.FOR, which was written to acquire intermittency data using the traverse mechanism described by Shayesteh and Bradshaw (1987). The technique of marking turbulent fluid in a boundary layer with heat by heating the boundary layer upstream has been described by Murlis, Tsai and Bradshaw (1982). Use of a cold-wire resistance thermometer allows the turbulent hot fluid to be distinguished from the cold freestream fluid, so that turbulence statistics obtained with a hot-wire in the intermittent region of a boundary layer can be conditioned on whether or not the fluid at a given instant is within the laminar/turbulent interface. This program was written so that measurements of the intermittency function (the fraction of time the fluid is turbulent in an intermittent region) can be made in a suitably heated flow.

D.2 Instrumentation Requirements

This program has been written for use with the Advance 86B (IBM PC compatible) computer and Tecmar Labmaster data acquisition system described in the report by Subramanian and Bradshaw (1985). The traverse mechanism is controlled using the computer parallel out port and three PHI modules as described in Section A.2, one for y-movement, one for yaw and one for pitch. The cold wire, which lies in the x-z

plane, is carefully positioned in the probe holder so that movement of the mechanism in pitch or yaw produces no movement of the probe tip in space. It is connected to the Platypus low-noise amplifier (see Bradshaw, 1976), and the output from this, which is a.c. coupled and proportional to temperature, goes directly to the Tecmar A/D converter.

D.3 Program Layout

When the program is executed, the user is presented with the following list of Options.

- 1 - Initialise traverse gear;
- 2 - calibrate cold-wire at reference location;
- 3 - move the probe;
- 4 - do a traverse in the y-direction;
- 5 - output the data to file;
- 6 - new run;
- 7 - stop.

Options 1, 3, 6 and 7 are the same as in Section B.3.

If Option 2 is chosen, the program obtains a reference temperature difference T_{ref} , and thence assigns T_1 , the temperature (measured relative to the cold inviscid fluid temperature) above which the fluid is to be assumed turbulent and below which it is assumed to

be non-turbulent. The user is first requested to input n_p , the number of samples used to form the averages, typically from 2000 to 10000. The choice is given of inputting T_{ref} (in units of Platypus output voltage) at the terminal or have the program determine it from measurements of the flow. If the user wishes the computer to determine it, the probe should be located in an intermittent region of the flow and the program will take n_p voltage samples from the Platypus. The maximum and minimum voltages are found and all the voltage samples within one percent of the difference are averaged to find an "average" maximum voltage (corresponding to cold-fluid temperature T_c , the output voltage increasing as temperature decreases) and an "average" minimum voltage (corresponding to a hot-fluid temperature T_h). The reference temperature rise (in units of Platypus output voltage) is given by $T_{ref} = T_h - T_c$. Finally, the user is requested to input the fraction T_1/T_{ref} and T_1 is calculated.

If Option 4 is chosen, the user is requested to input a series of y , yaw and pitch angles at the terminal, or the program can read this information from a disc file as described in Section B.3. The probe is then traversed thorough a sequence of y positions and at each y is approximately aligned with the local mean flow direction. Strictly speaking, the probe does not need to be aligned with the flow: however it is likely that a large misalignment would cause the traverse mechanism to interfere with the flow. After alignment, n_p Platypus voltage samples are obtained, the maximum voltage is found and all the samples within one percent of T_{ref} of this are averaged to obtain a minimum temperature for the cold "inviscid" region, T_0 . The fraction

of the data with a voltage below $T_i = T_0 + T_1$, that is with a temperature above the temperature of the interface between the cold "inviscid" fluid and the hot "turbulent" fluid, the intermittency I , is determined, as is the average temperature within the cold and hot regions of the fluid, T_c and T_h . Finally, the distance y , the intermittency I , and the non-dimensional temperature difference $(T_h - T_c)/T_{ref}$ are added to the results array. Note that the average, unconditioned, temperature of the fluid is given by the expression $(T_{ave} - T_c)/T_{ref} = I(T_h - T_c)/T_{ref}$.

If Option 5 is chosen, the program outputs the contents of the results array to a disc file.

Appendix E

The Second Traverse Mechanism

This Appendix describes the second traversing mechanism used for the data acquisition described in the main body of the report. This has motorised y, yaw and roll movements, but, unlike the traverse gear described by Shayesteh and Bradshaw (1987), lacks pitch movement.

The traverse mechanism is based on that used by Baskaran and Bradshaw (1987), which is designed to fit in a standard 88.9 mm socket in the working section wall. This mechanism is of a simple slide rule type with a seven inch movement powered by a servo motor and with a linear potentiometer for feedback of the probe position. A pin-wheel roll mechanism powered by a servo motor and with a 10 turn rotary potentiometer is mounted on the body of the traverse mechanism. It is connected by a long (400 mm) timing belt to the probe holder which it rotates in increments of exactly 45 degrees. Because of the relatively long timing belt and as a consequence of the slight elasticity of the timing belt, the backlash in the roll mechanism is a little greater than for the mechanism described by Shayesteh and Bradshaw (1987), and so the positional uncertainty in roll is also a little greater.

Instead of mounting the above mechanism in a 88.9 mm standard wall socket, it is mounted in a socket in a yaw mechanism so that the probe stem is parallel to the yaw axis but offset by about 83 mm. The probe is adjusted in its holder (which is at right-angles to the probe stem) so that the probe tip lies at the yaw axis. The 88.9 mm socket

in the yaw mechanism is attached rigidly to a 177.8 mm standard disc and this lies in a socket in which it can rotate and which forms part of working section wall panel. The periphery of the disc is toothed and meshes with a pinion on the yaw motor shaft and a separate pinion on a 10 turn potentiometer for yaw angle readout. Both the motor and the potentiometer are mounted rigidly to the socket. The yaw mechanism is similar to that described by Shayesteh and Bradshaw (1987).

Appendix F

Probe Descriptions

The pitot probe designed for use with the traverse mechanism described by Shayesteh and Bradshaw (1987) is a simple straight tube of diameter 1.25 mm. The method of data acquisition with this probe is described in Appendix B.

The three-tube probe designed for use with the traverse mechanism described in Appendix E is of the type shown in Figure 46(d) of Bryer and Pankhurst (1971). This probe has three tubes of diameter 0.84 mm which are soldered together in the plane of yaw; a central tube with forward-facing tip and a tube either side whose tip is chamfered at 45 degrees. The probe tip is offset from the traverse mechanism roll axis so that the tip can make contact with the test surface before the heel of the traverse mechanism probe stem does. The tubes of the probe incline down toward the wall at a small angle (2 to 4 degrees) so that the probe tip (rather than some other part of the probe) is guaranteed to touch the wall. The method of data acquisition with this probe is described in Appendix C.

The crossed hot-wire probe was manufactured in-house. The wires are soldered to the tips of two pairs of stainless steel prongs which are about 13 mm long, 3.2 mm apart in the y_w direction (see Figure A.2), and 1.6 mm apart in the z_w direction. The pair of prongs are of different lengths, so that the wires, when soldered to the tips of the

prongs, lie at +45 degrees to the flow direction and appear to cross (when viewed from the side) at their midpoint. The wires are manufactured from 0.005 mm diameter platinum-core Wollaston wire with a measurement region roughly 0.8 mm long etched in the middle (giving a cold resistance of about 6 Ohms). The method of manufacture of the wires is described by Bradshaw (1973). The method of data acquisition with this probe is described in Appendix A.

The cold-wire temperature probe has two stainless steel prongs about 13 mm long and 3.2 mm apart. Soldered to the tip is a 0.001 mm platinum-core Wollaston wire with a 0.8 mm long measurement length etched in the middle (giving a cold resistance of about 100 Ohms). The method of data acquisition with this probe is described in Appendix D.

Appendix G

The Effect of Instantaneous Velocity Gradients on Mean Velocity and Turbulence Statistics Measured With a Crossed Hot-wire Anemometer.

When using a crossed hot-wire anemometer to make measurements in a turbulent flow, it is usually assumed that the two wires are at effectively the same position in space. Thus, instantaneous gradients of velocity are sufficiently small that the two wires make measurements of effectively the same element of fluid. However, if we are not able to make such an assumption, but we are able to assume that gradients are sufficiently small that a given wire measures the velocity of the element of fluid at the wire centre, then we are able to make some corrections for the effect of wire spacing.

Figure A.2 defines the x_p, y_p, z_p (probe) and the x_w, y_w, z_w (wire) coordinate systems we use, and the roll positions 0, 1, 2, and 3. The wire angles 1 and 2 are assumed to be exactly 45 degrees and the wire spacing is Δ , so that the wire at $z_w = -\Delta/2$ measures (in effect) the instantaneous velocity $u_w + v_w$ and the wire at $z_w = \Delta/2$ measures (in effect) the instantaneous velocity $u_w - v_w$. It is easy to show that, neglecting terms of order Δ^2 or greater, the method for deriving u_p, v_p, w_p described in Section A.5 gives us in fact $u_{p,m}, v_{p,m}$ and $w_{p,m}$, defined by the equations below:

$$\text{Roll position 0; } u_{p,m} = u_p - \Delta/2 \partial v_p / \partial z_p$$

$$v_{p,m} = v_p - \Delta/2 \partial u_p / \partial z_p$$

$$\text{Roll position 1; } u_{p,m} = u_p + \Delta/4 (\partial(v_p + w_p) / \partial y_p - \partial(v_p + w_p) / \partial z_p)$$

$$(v_p + w_p)_m / \sqrt{2} = (v_p + w_p) / \sqrt{2} + \Delta / (2\sqrt{2}) (\partial u_p / \partial y_p - \partial u_p / \partial z_p)$$

$$\text{Roll position 2; } u_{p,m} = u_p + \Delta/2 \partial w_p / \partial y_p$$

$$w_{p,m} = w_p + \Delta/2 \partial u_p / \partial y_p$$

$$\text{Roll position 3; } u_{p,m} = u_p + \Delta/4 (\partial(-v_p + w_p) / \partial y_p + \partial(-v_p + w_p) / \partial z_p)$$

$$(-v_p + w_p)_m / \sqrt{2} = (-v_p + w_p) / \sqrt{2} + \Delta / (2\sqrt{2}) (\partial u_p / \partial y_p + \partial u_p / \partial z_p)$$

Let us assume that the effect of gradients is generally small (that is Δ is effectively zero) except in a boundary layer type of region where we may not ignore gradients with respect to y . If we use these equations to form the statistical averages described in Section A.5 then we obtain the following:

$$U_{p,m} = U_p + \Delta/4 \partial W_p / \partial y_p$$

$$V_{p,m} = V_p$$

$$W_{p,m} = W_p + \Delta/2 \partial U_p / \partial y_p$$

$$\overline{u^2}_{p,m} = \overline{u^2}_p + \Delta/2 \overline{u_p \partial w_p / \partial y_p}$$

$$\overline{v^2}_{p,m} = \overline{v^2}_p$$

$$\overline{w^2}_{p,m} = \overline{w^2}_p + \overline{w_p \partial u_p / \partial y_p}$$

$$(\overline{uv})_{p,m} = (\overline{uv})_p$$

$$(\overline{uw})_{p,m} = (\overline{uw})_p + \Delta/4 \partial (\overline{u^2}_p + \overline{w^2}_p) / \partial y_p$$

$$(\overline{vw})_{p,m} = (\overline{vw})_p + \Delta/2 \overline{v_p \partial u_p / \partial y_p}$$

We have not derived the expressions for the triple products, but these are likely to be complicated and contain terms that are difficult to measure.

Inspection of the above equations show that, in a boundary layer type of flow, the error in W_p and in $(\overline{uw})_p$ is likely to be significant, but that we can easily make a correction since the quantities which occur in the error term are all easily measurable. The error term in the equations for $\overline{u^2}_p$ and $\overline{w^2}_p$ cannot be easily evaluated, but is likely to be small as a percentage of $\overline{u^2}_p$ and $\overline{w^2}_p$ and so may be neglected. The error term in the equation for $(\overline{vw})_p$ may not be small as a percentage of $(\overline{vw})_p$ since $(\overline{vw})_p$ itself is small, but it should be remembered that $(\overline{vw})_p$ is already a rather uncertain quantity, being the difference between two relatively large experimentally determined quantities, so the additional contribution to the error may still be unimportant.

Figures G.1 and G.2 show the effect of making the above described corrections on $W_{p,m}$ and $(\overline{uw})_{p,m}$ to give W_p and $(\overline{uw})_p$. The data is from the "delta-wing high" case described in the main body of this report at $x/s = 667$ from the leading edge of the test plate and $z = 0$. The flow is symmetrical about the plane formed by $z = 0$ and the y axis, so that we require $W = 0$ and $\overline{uw} = 0$, a condition that is not satisfied by our results in the thin boundary layer, but is satisfied above it. The application of corrections gives $W = 0$ and $uw = 0$ in the boundary layer as well, as we expect and a similar improvement is obtained at other x positions ($x/s = 1.523, 3.238$ and 4.952) on the line $z = 0$. The correction was also applied to data for a normally developed two-dimensional boundary layer about 30 mm, but the error itself in this case was small and application of the correction produced little improvement.

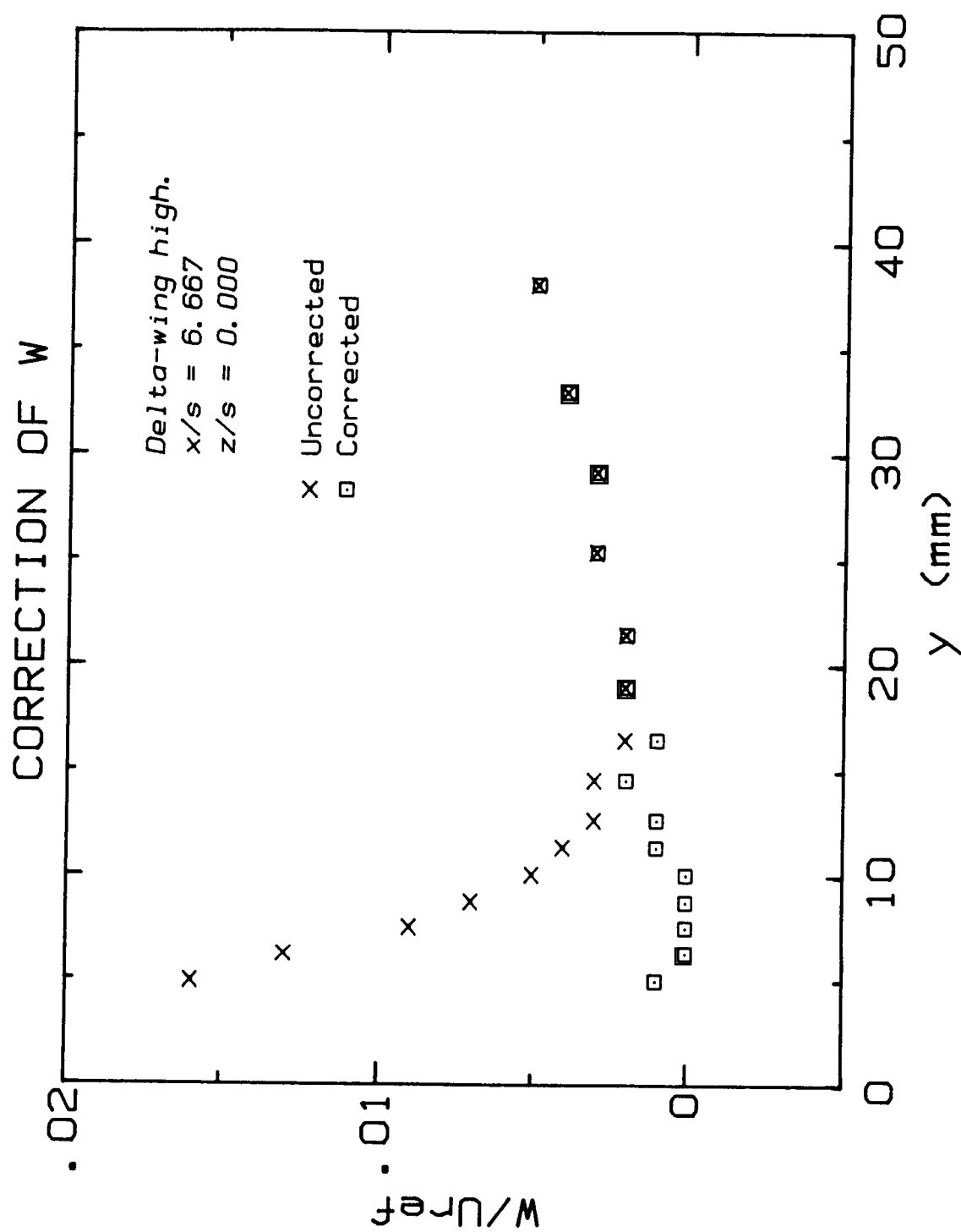


Figure G.1 Correlation of W for vertical separation of crossed wires

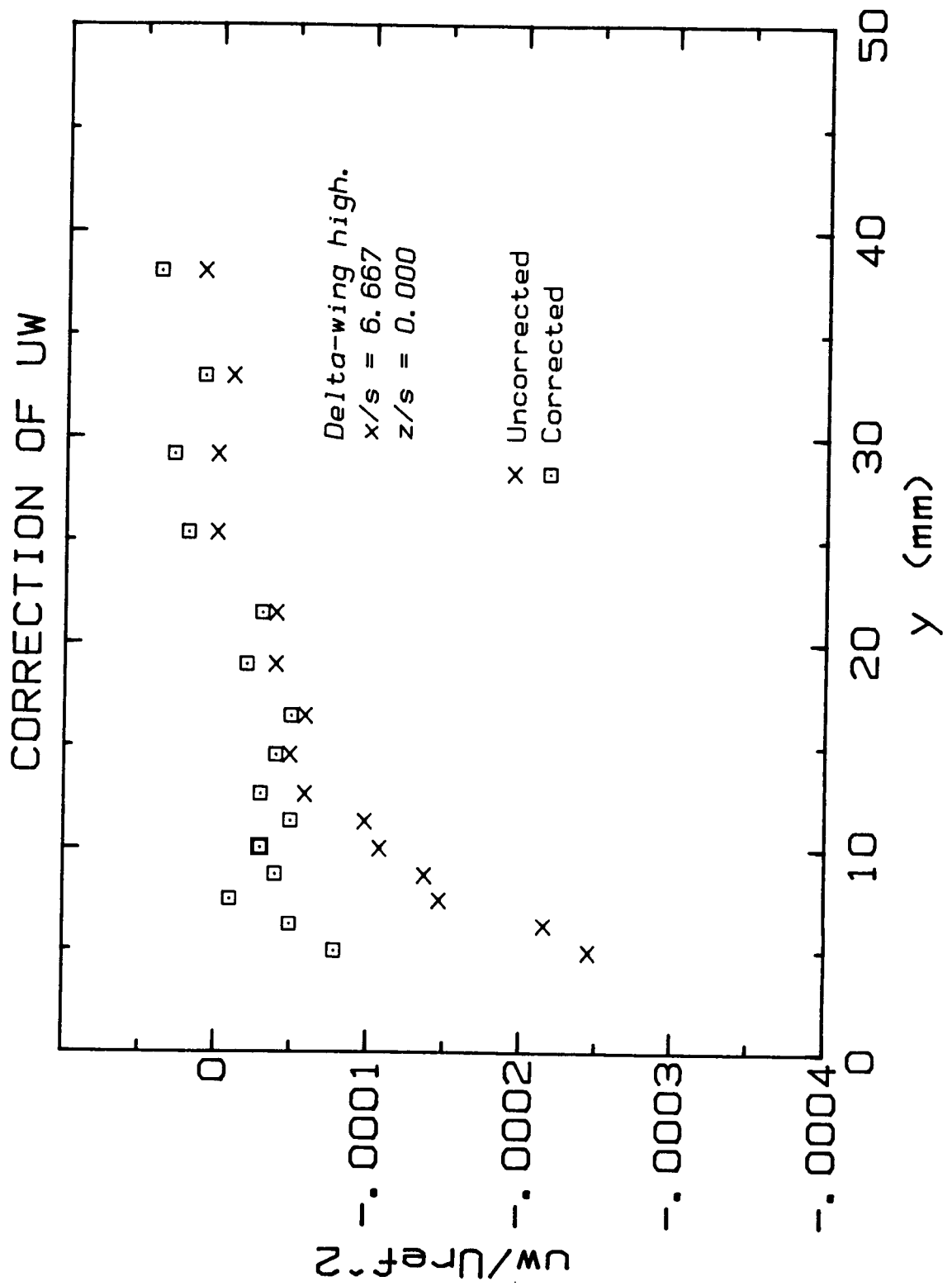


Figure 6.2 Correlation of uw for vertical separation of crossed wires

Appendix H

Traverse Mechanism Interference and Experimental Uncertainties

The traverse mechanism described by Shayesteh and Bradshaw (1987) has a relatively large probe-carrying head as a consequence of the pitch gear mechanism. It was feared that this might produce flow interference in the experiments described in the main body of this report, particularly since vortex bursting, which is a very large change in the vortex structure (see Leibovich, 1978), can often be precipitated by a small perturbation of the flow such as might be produced by a probe. To check whether this might be a problem, we introduced kerosene vapour smoke into the core of the vortex in the "delta-wing low" case so that the centre of the vortex was marked by the smoke to a diameter of about 10 mm. Note that smoke introduced into the core in this way does not diffuse out of the core, so that the vortex centre can be accurately followed for a large distance downstream. The traverse mechanism carrying a hot-wire probe was traversed (at $x/s = 3.238$) so that the probe tip passed through the center of the vortex, and it was clearly seen that the vortex upstream and in the immediate vicinity of the probe tip was not affected at all by the presence of the probe or the pitch mechanism. In fact, the vortex was not susceptible to bursting, at least not without applying a very large perturbation to the flow.

Additional checks for traverse mechanism pitch-head interference included the comparison of hot-wire profiles in a normally developed two-dimensional boundary layer with data obtained (at the same point)

using the traverse mechanism described in Appendix E. The agreement between these profiles was good, and well within the expected experimental error attributable to other sources. Comparison between hot-wire data and three-tube pressure probe data for both the "delta-wing low" case and the "delta-wing high" case show excellent agreement. However, it should be noted that in the "delta-wing low" case, small discrepancies in U were observed in the vicinity of the "tongue" of turbulent fluid which indicated a displacement of the origin of the z coordinate by 2 or 3 mm (a little greater than the expected error in the z position) between the three-tube probe and the hot-wire probe data sets.

The accuracy of our hot-wire data is probably a little better than the estimates given by the report on "Hot-Wire Anemometry at Low Mach Numbers" in Kline et al. (1981) for crossed hot-wires assuming good practice. Thus, the likely uncertainties (we quote all uncertainties at 20:1 odds) are; $U_w < \pm 2$ percent; $V_w = \pm 1$ percent of U_w (our estimate); $\overline{u_w^2}, \overline{v_w^2} < \pm 15$ percent; and ± 5 percent $< (\overline{uv})_w < \pm 15$ percent. The smoothness of the data shown in figures in the main body of the report indicate that the data are of good quality and that, at any rate, the random element of the uncertainty is much smaller than suggested by the above estimates. We are not able to provide an estimate of the uncertainty in the triple products, nor the uncertainty in $(\overline{vw})_p$, a quantity which is obtained by combining measurements from two different roll angles and whose uncertainty is therefore rather larger than the uncertainties in the above quantities.

The uncertainty in measurements of total pressure with the three-tube probe or the pitot are probably of the order of ± 2 percent, as are the measurements of wall static pressure coefficient, leading to an uncertainty in velocity deduced from the total pressure and wall static pressure (assuming no y gradient of static pressure) of ± 1.5 percent. Uncertainty in yaw angle measured with the three-tube probe is ± 0.5 degrees.

We estimate the uncertainty in probe positioning by the traverse mechanism of Shayesteh and Bradshaw (1987) to be ± 0.5 mm ± 0.5 percent in y and an additional (± 1 mm/45 degrees) per degree of pitch as a result of the probe tip not lying exactly on the axis of pitch; ± 0.2 degrees ± 1 percent in pitch; ± 0.2 degrees ± 0.5 percent in yaw; ± 3 degrees in roll. For data acquisition with the traverse mechanism described in Appendix E we estimate ± 0.5 mm ± 0.5 percent in y , ± 0.2 ± 0.5 percent in yaw; ± 3 degrees in roll. For data acquisition with the three-tube pressure probe using the traverse mechanism described in Appendix E, when particular care is taken in finding the wall, we estimate ± 0.025 mm ± 0.5 percent in y . The positional uncertainty in z is ± 1 mm in locating either of the above traversing mechanisms and an additional (± 2 mm/45 degrees) per degree of yaw angle as a result of the probe tip not lying exactly on the axis of yaw.

Appendix I

Boundary Layer Type Analysis of Three-Tube Pitot Data

This Appendix describes the analysis of the data obtained by the method described in Appendix C, in which a three-tube pitot probe is traversed in a boundary layer and at each point aligned with the local flow direction. The program reads data from the disc files written by the data acquisition program (which are in a standard format), and writes the results to disc.

In order to use this program, a reference profile must have been obtained in a two-dimensional boundary layer (ie. $\theta_y = 0$) of similar thickness to the profiles to be analysed, using an identical probe configuration and technique. The reference profile is used to correct for a small lack of symmetry in the probe which results in the measurement of a yaw angle which, although it is zero away from the wall where the probe was calibrated, is non-zero as the probe approaches to within a few probe tube diameters of the wall ($y < 5D$). This effect is assumed to be dependent only on the distance from the wall so that the correction is simply a subtraction from the measured yaw angle of the yaw angle interpolated from the reference profile to the current y position. This correction is small for the data reported in the main body of this report, being less than 1 degree, and we estimate that the resulting (corrected) yaw angle is accurate to within ± 0.5 degrees.

The program determines the U and W component mean velocities from the total pressure coefficient, the wall static pressure coefficient (assuming the static pressure remains constant across the boundary layer) and the yaw angle.

Skin friction coefficient is determined by fitting the resultant mean velocity (Q) to the logarithmic law of the wall, $Q/q_t = 1/0.41 \ln(y^+) + 5.2$, where $y^+ = yq_t/\nu$ in the range $50 < y^+ < 150$. The constants in the law of the wall are those recommended by de Brederode and Bradshaw (1974) and the method of fit is that described by Gillis and Johnston (1983). Pierce, McAllister and Tennant (1983) show, by comparison of direct measurements of the skin friction with measured mean velocity profiles, that this simple representation of the near wall resultant velocity distribution is as good as any other for a three-dimensional boundary layer with monotone increasing skew angle up to about 15 degrees. These authors suggest that, under the conditions described above, the accuracy of the magnitude of the skin friction coefficient determined by fit to the law-of-the-wall is of the order of ± 5 to 10 percent. The yaw angle of the skin friction vector ($\theta_{y,w}$) is assumed to be the yaw angle of the velocity vector for the first data point away from the wall. Inspection of profiles of mean velocity yaw angle, and extrapolation to the wall by eye, suggest that the uncertainty in this estimate should be no more than ± 1 degree.

A free-stream resultant velocity Q_e , which is the average resultant velocity for all the points which are within 0.5 percent of

the maximum, is found. From this the boundary layer 99.5 percent thickness (δ_{995}), the value of y (nearest the wall) where $Q = 0.995Q_e$, is found by linear interpolation of the data. The outer limit of integration (y_e) used in determining the integral parameters is $1.2\delta_{995}$ or y for the last data point, whichever is the smaller. The yaw angle at y_e ($\theta_{y,e}$) is determined by linear interpolation of the data, and the data are resolved into a streamline coordinate system where $U_s = Q \cos(\theta_y - \theta_{y,e})$ and $W_s = -Q \sin(\theta_y - \theta_{y,e})$. We add the point at the wall, $y = 0$, $U_s = 0$, $W_s = 0$, and interpolate a number of points between $y = 0$ and the first measured point (at $y > D/2$) using an expression derived by Spalding (1961) and the above mentioned constants, which may be written

$$y^+ = u^+ + \exp(-0.41 \times 5.2)(\exp(0.41u^+) - 1 - 0.41u^+ - (0.41u^+)^2/2 - (0.41u^+)^3/6).$$

This is solved for y^+ as a function of u^+ from which we get $U_s = u^+ u_t$ and $W_s = 0$ as a function of y . Finally, we determine the following integral thicknesses (from Cousteix, 1982) by quadrature of cubic spline fits to the quantities within the integral signs.

$$\delta_1 = \int_0^{y_e} (1 - U_s/Q_e) dy, \quad \delta_2 = \int_0^{y_e} W_s/Q_e dy, \quad \theta_{11} = \int_0^{y_e} U_s/Q_e (1 - U_s/Q_e) dy,$$

$$\theta_{21} = \int_0^{y_e} W_s U_s/Q_e^2 dy, \quad \theta_{12} = \int_0^{y_e} W_s/Q_e (1 - U_s/Q_e) dy, \quad \theta_{22} = \int_0^{y_e} (W_s/Q_e)^2 dy.$$

The results are output to disc files, with a separate file for each profile analysed which contains y , θ_y , Q and other information for each data point tabulated in a self-explanatory way. At the end of running the analysis program a file is output which tabulates the x , z position, skin friction coefficients, integral thicknesses, Reynolds numbers and other boundary layer parameters for all the profiles analysed by the program.

Appendix J

Hot-wire Data Analysis Programs

J.1 Introduction

This Appendix briefly describes a number of FORTRAN programs which have been written to obtain derived quantities from planes of hot-wire data. These include programs to evaluate the longitudinal vorticity and the cross-stream diffusion of longitudinal vorticity, the eddy viscosity, the turbulent energy balance and the Reynolds stress balances. Hot-wire data, including all mean velocity components, Reynolds stresses and triple products is read from disc files with the data format described in Appendix K, and the results are then written to disc files with a data format which is also described in Appendix K.

J.2 Longitudinal Vorticity and Turbulent Diffusion

The transport equation for the longitudinal vorticity (ω_1) can be written in tensor notation as

$$U_i \partial \omega_i / \partial x_i = \omega_i \partial U / \partial x_i + \nu \partial^2 \omega_1 / \partial x_i^2 + \partial \phi_i / \partial x_i,$$

where $x_1 = x$, $x_2 = y$, $x_3 = z$, $u_1 = u$, $u_2 = v$, $u_3 = w$, $U_1 = U$, $U_2 = V$,

$U_3 = W$, $\omega_i = e_{ijk} \partial U_j / \partial x_k$, and

$$\phi_i = \partial (\overline{u_1 u_2} - \delta_{i2} \overline{u_1^2} / 3) / \partial x_3 - \partial (\overline{u_1 u_3} - \delta_{i3} \overline{u_1^2} / 3) / \partial x_2.$$

We have chosen to write the turbulent diffusion terms in this manner since, for an isotropic eddy viscosity given by

$$\epsilon = \epsilon_{ij} = -(u_i u_j - \delta_{ij} \overline{u_1 u_1} / 3) / (\partial u_i / \partial x_j + \partial u_j / \partial x_i),$$

we may write $\phi_i = -\epsilon \partial \omega_1 / \partial x_i$.

This means, if the eddy viscosity is isotropic, that vectors plotted in the crossflow plane with component ϕ_2 in the x_2 direction and ϕ_3 in the x_3 direction will be normal to contours of the longitudinal vorticity (ω_1), and point down the gradient. Plotting the data in this way therefore provides a simple check of the validity of an isotropic eddy viscosity model.

The program VDIFF.FOR evaluates the terms ω_1 , ϕ_1 , ϕ_2 , ϕ_3 , and $\partial \phi_i / \partial x_i$ for a plane of data and outputs the results to a data file. The term $\partial \phi_1 / \partial x_1$, which should be small relative to the other diffusion terms, and the other terms in the transport equation are not evaluated because of the difficulty of obtaining accurate x derivatives.

J.3. Preparing the Data for Programs Which Evaluate x Derivatives

A program called SETUP.FOR has been written to prepare planes of data for the programs described in the following sections. This

program inputs two planes of hot-wire data which must be sufficiently close together in x that the flow may be assumed to vary between them in a linear fashion, but sufficiently far apart that the differences between them will be much greater to the experimental uncertainty (since otherwise the uncertainty in the x derivatives will be high). The planes of data must have equal numbers of traverses, and the k 'th traverse of plane 1 and the k 'th traverse of plane 2 must be either at the same z , or sufficiently close that the data may be assumed to vary in a linear fashion between them.

The program then fits the data for the k 'th traverse in plane 2 with a cubic spline and interpolates points to the y locations of the k 'th traverse of plane 1. Obviously, the data for the k 'th traverse of plane 2 must extend either side of the data for the k 'th traverse of plane 1. Finally, data for plane 3, a plane half-way between planes 1 and 2, is linearly interpolated so that (for the j 'th point of the k 'th traverse) a quantity Q at $y_{3,j,k} = y_{1,j,k} = y_{2,j,k}$ and $z_{3,j,k} = (z_{1,j,k} + z_{2,j,k})/2$ is given by $Q_{3,j,k} = (Q_{1,j,k} + Q_{2,j,k})/2$. Data files for planes 1, 2 and 3 are then output in a simple format for reading by further data analysis programs.

J.4. Eddy Viscosity

A program called EDDYV.FOR has been written which reads data for planes 1, 2 and 3 from disc files created as described in Section J.3 and calculates the six eddy viscosity coefficients (ϵ_{ij}) from the

expression given in Section J.2. All coefficients are evaluated for each k,j of plane 3, and the results, including the six strain rates given by $(\partial U_i/\partial x_j + \partial U_j/\partial x_i)$, are output to a data file.

J.5. Turbulent Kinetic Energy Balance

The turbulent kinetic energy equation in tensor notation is

$$\begin{aligned} \partial(\overline{U_k \overline{u_i u_i}}/2)/\partial x_k + \partial(\overline{u_k \overline{u_i u_i}}/2 + \overline{p/\rho u_k} - \partial(\overline{u_i u_i}/2)/\partial x_k)/\partial x_k \\ + \overline{u_i u_k} \partial U_i/\partial x_k + (\partial \overline{u_i}/\partial x_k) (\partial \overline{u_i}/\partial x_k) = 0. \end{aligned}$$

or more simply, convection + diffusion + production + dissipation = 0. The equation TKEB.FOR determines the convection, production, and diffusion terms directly from the data for each k,j of plane 3. We assume that $\partial(\overline{p/\rho u_k} + \nu \partial(\overline{u_i u_i}/2)/\partial x_k)/\partial x_k$ (the pressure and viscous diffusion) is relatively small, and consequently may be neglected. The dissipation is then obtained by difference and all the terms of the balance are output to a disc file. The dissipation results are also output to a separate disc file for subsequent reading by the program RESBAL.FOR, described below.

J.6. Reynolds Stress Balances

If, as above, we neglect the viscous diffusion and pressure diffusion terms and assume that the dissipation is isotropic, then we may write the equations for the Reynolds stresses as follows:

$$\begin{aligned} \partial(\overline{U_k \overline{u_i u_j}})/\partial x_k + \partial(\overline{u_k \overline{u_i u_j}})/\partial x_k + (\overline{u_j u_k} \partial U_i/\partial x_k + \overline{u_i u_k} \partial U_j/\partial x_k) \\ + \overline{p/\rho} (\partial \overline{u_i}/\partial x_j + \partial \overline{u_j}/\partial x_i) + (2/3) \nu \delta_{ij} (\partial \overline{u_i}/\partial x_k) (\partial \overline{u_i}/\partial x_k) = 0. \end{aligned}$$

or convection + diffusion + production + (pressure-strain) + dissipation = 0.

The program RESBAL.FOR requires that a particular Reynolds stress be chosen by the user and then determines the convection, diffusion and production terms directly from the data for each j,k of plane 3. It then reads the dissipation data from a file generated TKEB.FOR, determines by difference the pressure-strain term and outputs the results to a disc file.

J.7. Obtaining the Derivatives and Smoothing the Results

All the programs described above have the following features in common:

(i) Derivatives of a quantity Q with respect to y are obtained by the following simple linear fit.

$$\begin{aligned} y_p &= y_{j-1,k} - y_{j,k}, \quad y_m = y_{j,k} - y_{j-1,k}, \\ Q_p &= Q_{j+1,k} - Q_{j,k}, \quad Q_m = Q_{j,k} - Q_{j-1,k}, \\ (\partial Q / \partial y)_{j,k} &= (y_m Q_p / y_p + y_p Q_m / y_m) / (y_m + y_p) \end{aligned}$$

(ii) Derivatives with respect to z are obtained in a similar fashion. If Q_{k+1} is the value of Q interpolated from the data for the $k+1$ 'th traverse to $y_{j,k}$, and Q_{k-1} is obtained in a similar

fashion from the $k-1$ 'th traverse, then

$$\begin{aligned} z_p &= z_{k+1} - z_k, \quad z_m = z_k - z_{k-1}, \\ Q_p &= Q_{k+1} - Q_{j,k}, \quad Q_m = Q_{j,k} - Q_{k-1}, \\ (\partial Q / \partial z)_{j,k} &= (z_m Q_p / z_p + z_p Q_m / z_m) / (z_m + z_p) \end{aligned}$$

(iii) Derivatives with respect to x are only obtained by programs for which data for planes 1, 2 and 3 have been input. A correction is made if the k 'th traverse for planes 1 and 2 are at slightly different z .

$$(\partial Q / \partial x)_{3,j,k} = (Q_{2,j,k} - Q_{1,j,k} - (\partial Q / \partial z)_{1,j,k} (z_{2,j,k} - z_{1,j,k})) / (x_{2,j,k} - x_{1,j,k}).$$

(iv) The quantity $Q_{j,k}$ is smoothed after every differentiation to obtain $R_{j,k}$.

$$R_{j,k} = (Q_{j,k} + (y_p Q_{j-1,k} + y_m Q_{j+1,k}) / (y_p + y_m) + (z_p Q_{k-1} + z_m Q_{k+1}) / (z_p + z_m)) / 3.$$

(v) Derivatives with respect to y for the first and last points in a given traverse, and derivatives with respect to z for first and last traverses are treated in a manner which is obvious, but slightly different to that in (iii).

Appendix K

Data Library

This Appendix describes the data available as files on floppy disc or magnetic tape, and the format in which the data is written. The x position and flow case is encoded into the name of most of the data files as a letter in the range from A to K. A letter from A to F indicates the "delta wing low" case, and from G to K indicates the "delta-wing high" case. The x/s positions (where s , the span of the delta-wing vortex generator, is 266.7 mm) are A = 4.952, B = 1.524, C = 0.095, D = 6.667, E = 3.238, F = 3.810, G = 3.238, H = 4.952, I = 6.667, J = 5.810, and K = 1.524.

All the data, unless specified otherwise, are non-dimensionalised on the reference velocity U_{ref} (nominally 16 m/s) and the reference length s . The reference velocity is measured with a pitot probe (P_{ref}) and a reference static tap (p_{ref}) at $x/s = 1.524$, $z/s = -1.429$ for the "delta-wing low" case, and at $x/s = 0.667$, $z/s = -1.429$ for the "delta-wing high" case.

The following data is written as a single data file for each plane of data and is available on magnetic tape written by a VAX or on IBM PC compatible 360K floppy discs.

The hot-wire data (available both on tape and on floppy disc) is written as a single file for a plane of data with traverses ordered from the highest z to the lowest z and each traverse ordered in

increasing y. The file names are simply PLANEA.DAT, to PLANEK.DAT. The following FORTRAN code will read the data from the file:

```

      READ(1,'(F14.8)') XST
      READ(1,'(I10)') NUMK
      DO 10 K=1,NUMK
      READ(1,'(I10)') NUMJ(K)
      DO 20 J=1,NUMJ(K)
      READ(1,30)      Z,Y,UB,VB,WB,U2,V2,W2,UV,UW,VW
      1      U3,V3,W3,U2V,U2W,UV2,UW2,V2W,VW2,UVW
30      FORMAT(20(F14.8,/),F14.8)
20      CONTINUE
10      CONTINUE

```

We define XST as the x position in inches; NUMK the number of traverses; NUMJ(K) as the number of points in the K'th traverse; Z and Y as the z and y locations of the point in inches; UB, VB, and WB as the mean velocities; U2, V2, W2, UV, UW, and VW as the Reynolds stresses; U3, V3, W3, U2V, U2W, UV2, UW2, V2W, VW2, and UVW as the triple products.

The pitot profiles obtained as described in Appendix B are available on floppy disc for the "delta-wing low" case only, and the file names are DLPA.DAT to DLPF.DAT. The following FORTRAN code will read the data:


```

      READ(1,'(F14.8') XST
      READ(1,'(I10)') NUMK
      DO 10 K=1,NUMK
          READ(1,'(I10)') NUMJ(K)
          DO 20 J=1,NUMJ(K)
              READ(1,30) Z,Y,DP
30          FORMAT(F11.7,2F10.6)
20          CONTINUE
10          CONTINUE

```

We define DP as $(P - p_{ref}) / (P_{ref} - p_{ref})$, where P is the total pressure.

Temperature intermittency profiles obtained as described in Appendix D are available on floppy disc at $x/s = 3.238$ for the "delta-wing low" case. The file INTBL.DAT contains data for which the boundary layer is heated at the leading edge of the plate, INTWNG.DAT contains data for which the delta-wing is heated by embedded resistance wires, INTTE.DAT contains data for which the fluid at the trailing edge of the delta-wing is heated and INTCOR.DAT contains data for which the vortex core is heated by a small spiral resistance just above the tip of the delta-wing. The following FORTRAN code will read the data:

```

      READ(1,'(F14.8') XST
      READ(1,'(I10)') NUMK
      DO 10 K=1,NUMK
          READ(1,'(I10)') NUMJ(K)
          DO 20 J=1,NUMJ(K)
              READ(1,30) Z,Y,INT,TEMP
30          FORMAT(F11.7,2F10.6)
20          CONTINUE
10          CONTINUE

```

We define $INT = I$, the intermittency; $TEMP = (T_h - T_c)/T_{ave}$, the non-dimensional temperature of the hot fluid relative to the cold fluid.

Other data are available on floppy disc. These data include the three-tube pitot profiles obtained as described in Appendix C at $x/s = 1.524, 3.238, 4.952$, and 6.667 for both "delta-wing low" case and "delta-wing high" case. The file names are as follows: PAP1.DAT, PAM1.DAT, ..., PBP1.DAT, PBM1.DAT, ...etc. The first letter of the file name is always P, the second is A to K indicating the x location, and the rest indicates the z location where P1 means $z = 1$ inch, M15 indicates $z = -15$ inches, and so on. Other files include PARAM1.DAT and PARAM2.DAT which are tabulated boundary layer parameters for respectively the "delta-wing low" case and the "delta-wing high" case obtained from the three-tube pitot profiles as described in Appendix I. These data files are too long to reproduce in this report. Both the contents of these files and the format in which the data are written

should be self evident to the user.

The quantities derived by the analysis programs described in Appendix J are written as a single data file for each plane of data. The results are available on magnetic tape written by a VAX.

The vorticity and turbulent diffusion of vorticity are available for the planes A, B, C, D, E, G, H, I, and K in the files VORTA.DAT, VORTB.DAT, etc. The following FORTRAN code will read the data from these files:

```

      READ(1,'(F14.8)') XST
      READ(1,'(I10)') NUMK
      DO 10 K=1,NUMK
        READ(1,'(I10)') NUMJ(K)
        DO 20 J=1,NUMJ(K)
          READ(1,30) ZZ,YY
          READ(1,40) VORT,VDIFF,VORTU,VORTV,VORTW,VB,WB
30      FORMAT(F11.6,F10.6)
40      FORMAT(F11.4,F10.5,5F10.6)
20      CONTINUE
10      CONTINUE

```

We define $ZZ = z/s$; $YY = y/s$; $VORT = x$; $VDIFF = \partial\phi_i/\partial x_i$; $VORTU = \phi_1$; $VORTV = \phi_2$; $VORTW = \phi_3$; $VB = V$; $WB = W$.

The coefficients of eddy viscosity are available for the "delta-wing low" case at $x/s = 3.524$ (derived from PLANEE.DAT and PLANEF.DAT) in the file VISC1.DAT and for the "delta-wing high" case at $x/s = 5.381$ (derived from PLANEH.DAT and PLANEJ.DAT) in the file VISC2.DAT. The following FORTRAN code will read the data from the file:

```

      READ(1,'(F14.8)') XST
      READ(1,'(I10)') NUMK
      DO 10 K=1,NUMK
        READ(1,'(I10)') NUMJ(K)
        DO 20 J=1,NUMJ(K)
          READ(1,30) ZZ,YY
          READ(1,40) V11,V22,V33,V12,V13,V23
          READ(1,50) S11,S22,S33,S12,S13,S23,Q2,VB,WB
30      FORMAT(F11.6,F10.6)
40      FORMAT(F13.8,5F12.8)
50      FORMAT(F9.4,5F8.4,F8.5,2F8.4)
20      CONTINUE
10      CONTINUE

```

We define $V_{11} = \epsilon_{11}$, $V_{12} = \epsilon_{12}$, etc.; $S_{11} = s_{11}$, $S_{12} = s_{12}$, etc. where $s_{ij} = \partial U_i / \partial x_j + \partial U_j / \partial x_i$; $Q2 = \overline{u^2} + \overline{v^2} + \overline{w^2}$.

The turbulent kinetic energy balance is available for the "delta-wing low" case at $x/s = 3.524$ (derived from PLANEE.DAT and

PLANEF.DAT) in the file ENERG1.DAT and for the "delta-wing high" case at $x/s = 5.381$ (derived from PLANEH.DAT and PLANEJ.DAT) in the file ENERG2.DAT. The following FORTRAN code will read the data from the file:

```

      READ(1,'(F14.8)') XST
      READ(1,'(I10)') NUMK
      DO 10 K=1,NUMK
        READ(1,'(I10)') NUMJ(K)
        DO 20 J=1,NUMJ(K)
          READ(1,30) ZZ,YY,CONV,DIFF,PROD,DISS
          READ(1,40) XDIFF,DISL,Q2,VB,WB
30      FORMAT(F11.6,F10.6,4F12.8)
40      FORMAT(F10.5,4F9.5)
20      CONTINUE
10      CONTINUE

```

We define CONV, DIFF, PROD, DISS as the convection, diffusion, production, and dissipation terms of the balance; XDIFF as the ratio

$$(\partial(\overline{u_1 u_i u_i}) / \partial x_1) / \text{convection}; \quad \text{DISL} = (\overline{u_1 u_2})^{3/2} / (\text{dissipation}).$$

The Reynolds stress balances are available for the "delta-wing low" case at $x/s = 3.524$ (derived from PLANE.E.DAT and PLANEF.DAT) and for the "delta-wing high" case at $x/s = 5.381$ (derived from PLANEH.DAT and PLANEJ.DAT). The file names are of the form RES12C1.DAT, where the first three letters are always RES, the two numbers which follow indicate the stress (in this case $\overline{u_1 u_2}$), the letter which follows is

always C and the final number indicates the case (1 indicating "delta-wing low" and 2 indicating "delta-wing high"). The following FORTRAN code will read the data from the file:

```

      READ(1,'(F14.8)') XST
      READ(1,'(I10)') NUMK
      DO 10 K=1,NUMK
        READ(1,'(I10)') NUMJ(K)
        DO 20 J=1,NUMJ(K)
          READ(1,30) ZZ,YY,CONV,DIFF,PROD,PSTR
          READ(1,40) XDIFF,Q2,VB,WB
30      FORMAT(F11.6,F10.6,4F12.8)
40      FORMAT(F10.5,3F9.5)
20      CONTINUE
10      CONTINUE

```

We define CONV, DIFF, PROD, PSTR as the convection, diffusion, production, and pressure-strain terms of the balance; XDIFF as the ratio

$$(\partial(\overline{u_1 u_1 u_j})/\partial x_1)/\text{convection}.$$

Appendix L

Colour Photographs

Upwards of seventy different photographs are available of a variety of hot-wire and derived data plotted as contours in the y,z plane. These were plotted on a colour monitor using a FORTRAN program which was developed by Professor John Eaton of Stanford University whilst on sabbatical at Imperial College, and the monitor was photographed. The program runs on the Imperial College Computer Centre VAX and is linked with DISSPLA, proprietary software package developed by ISSCO. A number of slightly different versions of the program were written, and these are;

DISDAT.FOR, for plotting mean velocities and Reynolds stresses in cartesian (x,y,z) coordinates.

DISCYL.FOR, for plotting mean velocities and Reynolds stresses in cylindrical (x,r,θ) coordinates. The data is converted from cartesian coordinates using the following expressions.

$$\overline{v_r^2} = \overline{v^2} \cos 2\theta + 2\overline{vw} \cos \theta \sin \theta + \overline{w^2} \sin^2 \theta,$$

$$\overline{v_\theta^2} = \overline{w^2} \cos^2 \theta - 2\overline{vw} \cos \theta \sin \theta + \overline{v^2} \sin^2 \theta,$$

$$\overline{uv_r} = \overline{uv} \cos \theta + \overline{uw} \sin \theta,$$

$$\overline{uv_\theta} = \overline{uw} \cos \theta - \overline{uv} \sin \theta,$$

$$v_\theta v_r = (\overline{w^2} - \overline{v^2}) \cos \theta \sin \theta + \overline{vw} (\cos 2\theta - \sin 2\theta),$$

where $\sin \theta = (z - z_c)/r$, $\cos \theta = (y - y_c)/r$, $r = \sqrt{(z - z_c)^2 + (y - y_c)^2}$,

and y_c, z_c is the location of the centre of the vortex (actually the position of the data point with the highest $\overline{q^2} = \overline{u^2} + \overline{v^2} + \overline{w^2}$).

DISVORT.FOR, for plotting longitudinal vorticity and $\partial\phi_i/\partial x_i$ (the turbulent diffusion term in the transport equation for longitudinal vorticity) from data derived by the program VDIFF.FOR (see Appendix J).

DISVISC.F, for plotting the eddy viscosity coefficients (ϵ_{ij}) derived by the program EDDYV.FOR (see Appendix J). This program leaves regions black for which the denominator in the term for the ϵ_{ij} , $\partial U_i/\partial x_j + \partial U_j/\partial x_i$, is less than a cutoff value which is input by the user at runtime. Thus, regions where ϵ_{ij} becomes very large but where the Reynolds stresses are not necessarily large are not shown.

DISENRG.FOR, for plotting terms of the turbulent kinetic energy equation derived by the program TKEB.FOR (see Appendix J).

In all versions of the program the grid of data is refined by linearly interpolating additional points (typically two or three) between each pair of points in a traverse and then interpolating additional traverses (typically two or three again) between traverse pairs. Each data point is then assigned to one of a number of colour bands of equal width according to the magnitude of the quantity being plotted, a square is drawn around the point whose sides lie halfway between the point and its neighbours, and the square is filled with the assigned colour. All the programs leave black those regions for which no data is available or where $q^2/2 < 0.0001$. The magnitude of the quantity plotted at the lower limit of the bottom colour band and at

the upper limit of the upper band are written next to the colour key (which gives the order of the colour bands) at the top of the plot. Finally, a black + is drawn at the vortex centre, the location of the data point with the highest $q^2/2$.

Photographs are available for the turbulent kinetic energy at $x/s = 0.095, 1.524, 3.238, 4.952$ and 6.667 for the "delta-wing low" case and at $x/s = 1.524, 3.238, 4.952$, and 6.667 for the "delta-wing high" case; for all the Reynolds stresses (in both cartesian and cylindrical coordinates) at $x/s = 0.095, 3.238$, and 6.667 for the "delta-wing low" case and at $x/s = 3.238$, and 6.667 for the "delta-wing high" case; the $\partial \Omega_i / \partial x_j$ term in the longitudinal vorticity equation at $x/s = 0.095, 1.524, 3.238, 4.952$, and 6.667 for the "delta-wing low" case; the turbulent kinetic energy equation convection, diffusion, production and dissipation terms at $x/s = 3.524$ for the "delta-wing low" case and at $x/s = 5.810$ for the "delta-wing high" case; the eddy viscosity coefficients $\epsilon_{12}, \epsilon_{13}, \epsilon_{23}$ at $x/s = 3.524$ for the "delta-wing low" case and at $x/s = 5.810$ for the "delta-wing high" case; the $\overline{v_r v_\theta}$ stress at $x/s = 6.667$ for the "delta-wing low" case with the stress derived using a vortex centre at $y_c, z_c + 0.025$ and $y_c, z_c + 0.1$ instead of at y_c, z_c . Individual copies of these photographs are available from the authors upon request.